Marine and Petroleum Geology 126 (2021) 104925

Contents lists available at ScienceDirect

Marine and Petroleum Geology

journal homepage: www.elsevier.com/locate/marpetgeo

Hydrocarbon-bearing sulphate-polymetallic deposits at the Colipilli area, Neuquén Basin, Argentina: Implications in the petroleum system modeling

Melisa A. Salvioli [a], Carlos A. Ballivián Justiniano [a], María F. Lajoinie [a], Hernán G. de la Cal [b], Remigio Ruiz [c], Nora N. Cesaretti [d], Mabel E. Lanfranchini [e,*]

[a] Consejo Nacional de Investigaciones Científicas y Técnicas (CONICET). Instituto de Recursos Minerales (INREMI), Universidad Nacional de La Plata–Comisión de Investigaciones Científicas de la Provincia de Buenos Aires. Calle 64 esquina 120, 1er piso, C.P. 1900, La Plata, Argentina
[b] ROCH S.A. Avenida Madero 1020, Piso 21, C.P. C1106ACX, Buenos Aires, Argentina
[c] Consejo Nacional de Investigaciones Científicas y Técnicas (CONICET). YPF Tecnología (Y-TEC). Avenida del Petróleo s/n, C.P. 1923, Berisso, Argentina
[d] Depto. de Geología, CGAMA–Universidad Nacional del Sur. San Juan 670, C.P. 8000, Bahía Blanca, Argentina
[e] Comisión de Investigaciones Científicas de la Provincia de Buenos Aires (CIC). Instituto de Recursos Minerales (INREMI), Universidad Nacional de La Plata–CIC. Calle 64 esquina 120, 1er piso, C.P. 1900, La Plata, Argentina

ARTICLE INFO

Keywords:
Barite-polymetallic mineralizations
Fluid inclusions
Hydrothermal fluids
Hydrocarbons
Thermal anomaly
Atypical petroleum system
Lower cretaceous
Agrio fold and thrust belt

ABSTRACT

This work deals with the hydrocarbon-bearing barite-polymetallic mineralizations of the Colipilli area, located in the western sector of the Agrio Fold and Thrust Belt (Neuquén Basin, Argentina). The mineralizations consist of bed- and vein-type deposits mainly composed of barite (barite$_{96.99\%}$–celestine$_{2.93\%}$) with minor amounts of Fe-oxyhydroxides and sulfides. The bed-type deposits have zebra texture and are emplaced along the contact between Late Cretaceous–Paleocene igneous rocks (Naunauco Group) and their Early Cretaceous sedimentary host rocks (*e.g.*, Huitrín Formation). In contrast, the vein-type deposits have breccia texture and are crosscutting the Mulichinco, Agrio and Huitrín formations or the andesitic/dioritic stocks and sills of the Naunauco Group. Different types and families of primary fluid inclusions (FI) were identified in the barite crystals. Fluorescence techniques with UV incident light and Raman spectroscopy allowed FI from completely aqueous to completely organic, including all the intermediate terms, to be identified. The organic FI have blue fluorescence and contain liquid hydrocarbons. The blue fluorescence is correlated with medium to high API gravity values (*ca.* 40°), indicating the presence of light hydrocarbons of advanced maturity related with the window for the generation of liquid/gaseous hydrocarbons. Microthermometry studies carried out on aqueous FI revealed that vein-type deposits formed at higher temperatures and salinities (249.7 °C and 0.5–9.3 wt % NaCl equivalent) than bed-type deposits (162.2 °C and 0.2–7.2 wt % NaCl equivalent). The heat influx provided by the Late Cretaceous–Paleocene magmatism promoted the circulation of inorganic and organic fluids of connate origin and the leaching of metallic and non-metallic elements from the sedimentary pile. During its crystallization, barite trapped fluids with variable hydrocarbon contents. The thermal anomaly associated with the magmatic activity could also have contributed with the maturation of the nearby source rocks and to the development of an atypical petroleum system.

1. Introduction

The Neuquén Basin, one of the most important hydrocarbon basins of Argentina (Fig. 1a and b), records a large sedimentation of Late Triassic–Paleogene age and an important tectono-magmatic activity of Cretaceous–Tertiary age; the latter mainly developed in the western sector of the basin. Several investigations related to hydrocarbon exploration have been carried out in the basin (*e.g.*, Carbone et al., 2018). Moreover, the wide distribution of barite-polymetallic mineralizations constitutes another important focus of study (*e.g.*, Brodtkorb et al., 1975; Hayase and Bengochea, 1975; de Barrio et al., 2014).

The oil discovery in Plaza Huincul in 1918, within the Neuquén Basin, triggered a long exploratory history (*e.g.*, Carbone et al., 2018). Thus, petroleum exploration provided great information to understand both sedimentary and tectonic evolution of the basin (*e.g.*, Cobbold and Rossello, 2003; Zamora Valcarce, 2007). On the other hand,

* Corresponding author.
E-mail addresses: lanfranchini@yahoo.com, mlanfranchini@fcnym.unlp.edu.ar (M.E. Lanfranchini).

https://doi.org/10.1016/j.marpetgeo.2021.104925
Received 3 July 2020; Received in revised form 21 December 2020; Accepted 8 January 2021
Available online 21 January 2021

geo-economic researches of barite deposits (Angelelli et al., 1976) allowed to define that the most important occurrences of barium and strontium in Argentina extend from southern Mendoza to southern Neuquén (Brodtkorb et al., 1975; Hayase and Bengochea, 1975; Llambías and Malvicini, 1978; de Barrio et al., 2014; Leal and Mateo, 2015). Additionally, more detailed genetic studies were performed for the Chorriaca, Bajada del Agrio, Continental, Mallín Quemado and Colipilli districts (Fig. 1b) (Brodtkorb et al., 1985; Llambías and Malvicini, 1978; de Barrio et al., 2014, 2016; Escobar, 2016; Salvioli, 2017). Two types of genesis were attributed to these mineralizations according to different authors: 1) related to the sedimentary environment of the host rocks (syngenetic processes; Brodtkorb et al., 1975) and 2) related to hydrothermal fluids (epigenetic processes; Hayase and Bengochea, 1975; Llambías and Malvicini, 1978; de Barrio et al., 2014; Escobar, 2016). Recent studies performed in barite crystals from the Chorriaca and Colipilli districts allowed the presence of rich-hydrocarbon fluid inclusions to be identified (Leal and Mateo, 2015; Salvioli et al., 2018).

The Colipilli area is a barite-rich district, located in the central-western portion of the Neuquén Basin (Fig. 1c). This sector differs from the rest of the neighboring barite districts due to the presence of outcrops of the carbonate-dominated Huitrín Formation of Early Cretaceous age, intruded and covered by the intrusive and extrusive

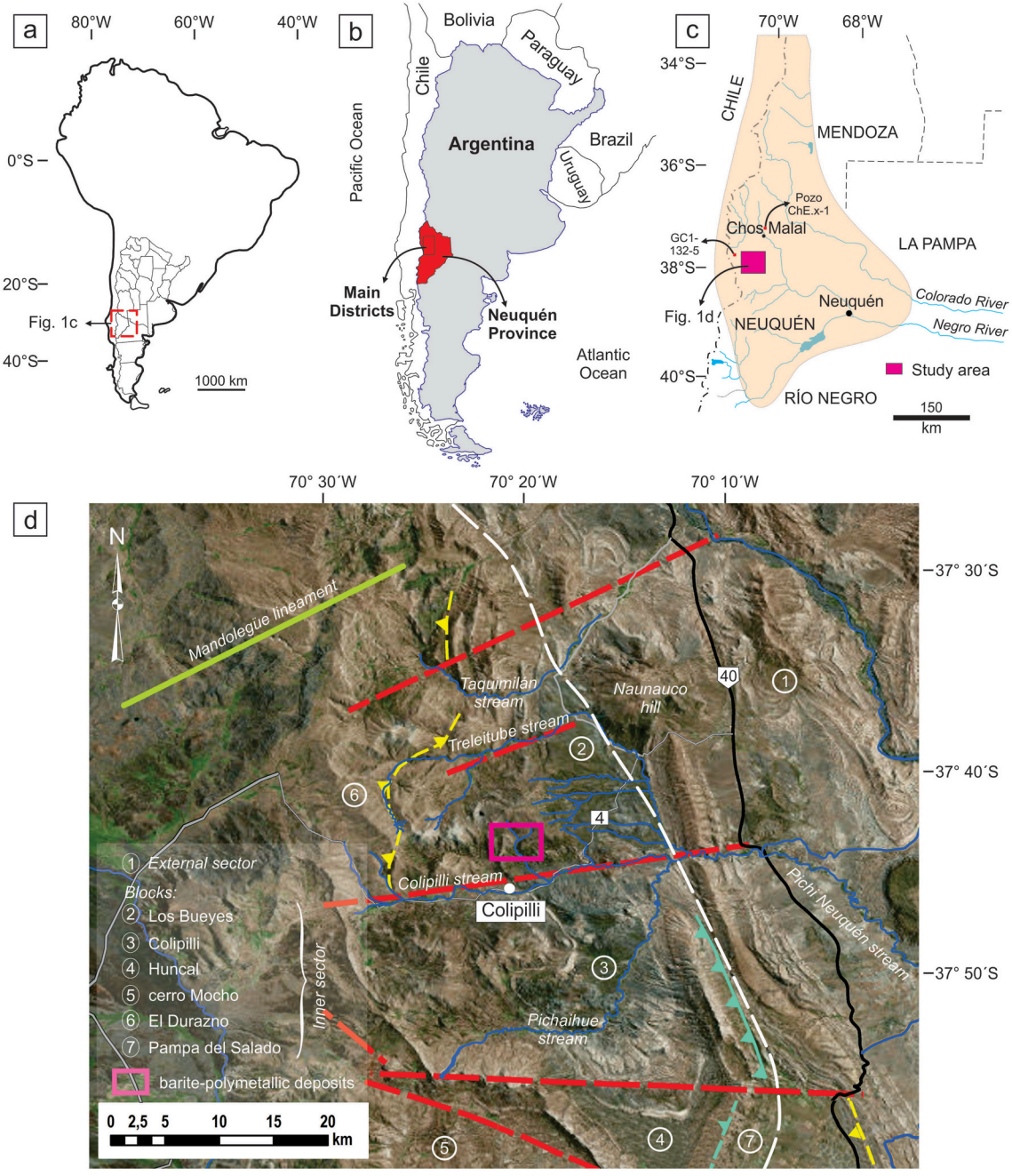

Fig. 1. a) Map of South America and political map of Argentina indicating the Neuquén Province. **b)** Map of Argentina indicating the Neuquén Province. **c)** Detail of the Neuquén Basin that includes the location of the Colipilli area (study area), the Chapúa Este well (ChE.x-1) and an apatite sample for fission track analysis (Rojas Vera et al., 2015) (see section 7.2). **d)** Satellite image of the Colipilli area indicating the location of the barite-polymetallic deposits and the geotectonic scheme of the area (Repol et al., 2002; Rojas Vera, 2011; Rojas Vera et al., 2015). **Legends:** red broken lines = pre-Liassic faults; yellow broken lines = pre-Liassic faults reactivated in near orthogonal directions; turquoise broken lines = reverse faults; white broken lines = inner-out deformation limit of the Agrio Fold and Thrust Belt. (For interpretation of the references to color in this figure legend, the reader is referred to the Web version of this article.)

intermediate rocks of the Naunauco Group of Late Cretaceous–Paleocene age (Zamora Valcarce, 2007; Salvioli, 2017; Salvioli et al., 2018). The barite-polymetallic mineralizations are spatially associated with these rocks and occur in two main morphological types: concordant and crosscutting the stratification (Fig. 1d).

Chemical analysis and microthermometry studies carried out in barite crystals from the Colipilli area are presented and discussed here. The main objective of these studies is to propose a genetic model for the Colipilli barite deposits that relates barite crystallization with its hydrocarbon-rich fluid inclusions. According to these investigations, the temperature rise of host rocks was by contact heat transfer related to thermal aureoles, which produced convective hydrothermal systems that promoted migration of oil and gases (*e.g.*, Rodríguez Monreal et al., 2009; Spacapan et al., 2020). Moreover, the convective hydrothermal systems could also have contributed to crack organic matter and transfer heat to large masses of rocks, generating a local thermal anomaly or increasing the regional thermal gradient. In this sense, the genetic model for the Colipilli barite deposits could have important implications both for the thermal evolution knowledge of the area and for contributing to adjust the petroleum system models of the Neuquén Basin proposed by other authors (*e.g.*, Rocha et al., 2018; Brisson et al., 2020).

2. Geological setting

2.1. Regional geology

The Neuquén Basin is located in central-western Argentina and extends along the Neuquén, Mendoza, Río Negro and La Pampa provinces (Fig. 1a and b). It was a large depocenter during the Late Triassic–Paleogene. The infill of the Neuquén Basin includes siliciclastic, carbonate and evaporate sedimentites of marine and continental origin that were progressively accumulated under different tectonic regimes (Howell et al., 2005).

The tectonic evolution of the basin records a complex history that includes a synrift stage (Late Triassic–Early Jurassic), followed by a long period of thermal subsidence in a retroarc setting (Early Jurassic–Early Cretaceous) and a final foreland basin development (Late Cretaceous–Cenozoic) (Vergani et al., 1995; Franzese and Spalletti, 2001; Howell et al., 2005).

During the sedimentation dominated by thermal subsidence and eustatic sea-level changes, the Cuyo (Dellapé et al., 1978), Lotena (Leanza, 1992), Mendoza (Stipanicic et al., 1968) and Bajada del Agrio (Méndez et al., 1995) groups were deposited. Due to their direct link with the Colipilli barite deposits, the Mendoza and Bajada del Agrio groups will be described in detail in Section 2.2. However, it should be noted that both groups are widely represented throughout the basin. Oil source rocks were identified in several of these units, like in the Los Molles Formation of the Cuyo Group or the Vaca Muerta and Agrio formations of the Mendoza Group (Weaver, 1931). Among them, the Vaca Muerta Formation has been identified as one of the most important conventional and unconventional shale resource targets of the basin, both for oil and gas (*e.g.*, Brisson et al., 2020). Likewise, important anhydride units, as those of the Auquilco (Lotena Group; Weaver, 1931) and Huitrín (Bajada del Agrio Group; Groeber, 1946) formations, were identified; they acted, together with black shales, as seal rocks and were the main detachment levels for thin-skin thrust sheets (Brisson, 2015).

During the Late Cretaceous, there was a renewal of the tectonic activity due to changes in the expansion rate of the ocean floor, which generated a positive reverse speed that gave rise to the foreland stage (Zapata and Folguera, 2006). The result was a compressive deformation stage with tectonic inversion of the previous extensional structures, correlated with a slight horizontalization of the subducted oceanic slab (Zamora Valcarce et al., 2011), that favored the deposition of the continental facies of the Neuquén Group (Legarreta and Uliana, 1991, 1999; Vergani et al., 1995; Franzese et al., 2003; Tunik et al., 2010). The stratigraphy of the Neuquén Basin ends with the siliciclastic and carbonate rocks of the Malargüe Group (Maastrichtian–Danian), which records the first Atlantic marine transgression related to the Western Gondwana break-up (*e.g.*, Aguirre-Urreta et al., 2011).

Towards the end of the Mesozoic, an important arc magmatism was developed along a north-south belt in the northwestern sector of the Neuquén province (Llambías and Aragón, 2011). Zamora Valcarce et al. (2006) assigned this magmatism, of Late Cretaceous–Paleocene age, to the Naunauco Group, which is integrated by the Colipilli (intrusive rocks; Llambías and Rapela, 1987, 1989) and Cayanta (extrusive rocks; Rapela and Llambías, 1985) formations. The igneous rocks of the Naunauco Group have intermediate compositions, an average K–Ar whole rock age of *ca*. 50 Ma (Llambías and Rapela, 1989) and Ar/Ar plagioclase ages of 72.83 ± 0.83 Ma, 65.50 ± 0.46 Ma and 56.64 ± 0.44 Ma (Zamora Valcarce et al., 2006).

A new deformation stage of Paleocene–Middle Miocene age reactivated numerous fold and thrust belts of the basin (Zamora Valcarce et al., 2006). This event is documented by the synorogenic deposits of the Tralalhué Conglomerate (Ramos, 1998). A last deformation stage could be inferred towards the end of the Miocene (Zamora Valcarce et al., 2006), during which the Tralalhué Conglomerate would have been elevated and tilted.

Finally, magmatic activity of Miocene age is represented by basalts and alkaline basaltic andesites in the north-central sector of the Neuquén province. Based on its chemical composition, these rocks were interpreted as products of intraplate volcanism developed during a retroarc extensional stage with little connection to the magmatic arc (Ramos and Barbieri, 1988; Kay and Copeland, 2006).

2.2. Local geology

The Agrio Fold and Thrust Belt (Ramos, 1978; Leanza et al., 2006) constitutes the structural context of the Colipilli area (study area). This morphostructural unit is characterized by two zones: a western zone where thick-skinned structures were formed as product of the tectonic inversion of faults that affected the basement, and an eastern zone where thin-skinned structures dominate (Fig. 1d) (Ramos, 1998; Zapata et al., 2002; Rojas Vera et al., 2015). The Colipilli area is included into the western zone, where the basement was exposed through a set of blocks limited in depth by pre-Liassic faults without superficial expression (Zapata and Folguera, 2006; Zamora Valcarce et al., 2009). These structures correspond to old inverted normal faults and transverse accommodation faults, both belonging to an old Jurassic extensional system reactivated during the Cretaceous–Tertiary compressive deformation stage (Vergani et al., 1995). As a result of these deep structures, several blocks known as Los Bueyes, Colipilli, Huncal, Cerro Mocho, El Durazno and La Pampa del Salado were exposed (Fig. 1d) (Ramos, 1998).

The most important morphostructural feature of the study area is the presence of folds. Synclines tend to be wide and flat while most anticlines are tight and upright, although some are recumbent. Fold wavelengths are variable, probably as a result of competition between thin-skinned and thick-skinned processes. The first works emphasized thin-skinned folding of “Chorriaca” style due to detachment on evaporate or shale levels (Bracaccini, 1970; Ramos, 1978), while recent works have focused on thick-skinned deformation (Ramos, 1998; Zapata et al., 1999).

The Colipilli area is mainly composed of Lower Cretaceous rocks of the Mendoza and Bajada del Agrio groups, separated from the Upper Cretaceous rocks of the Neuquén Group by a regional unconformity (Figs. 2 and 3) (Tunik et al., 2010).

The Mendoza Group is represented in the study area by the Vaca Muerta, Mulichinco and Agrio formations (Weaver, 1931). The organic matter-rich dark laminated pelites of the Vaca Muerta Formation are scarce and crop out in the nucleus of anticlines (for this reason they do not appear in Fig. 2). The light brown sandstones of the Mulichinco Formation also crop out in the nucleus of anticlines. The Agrio

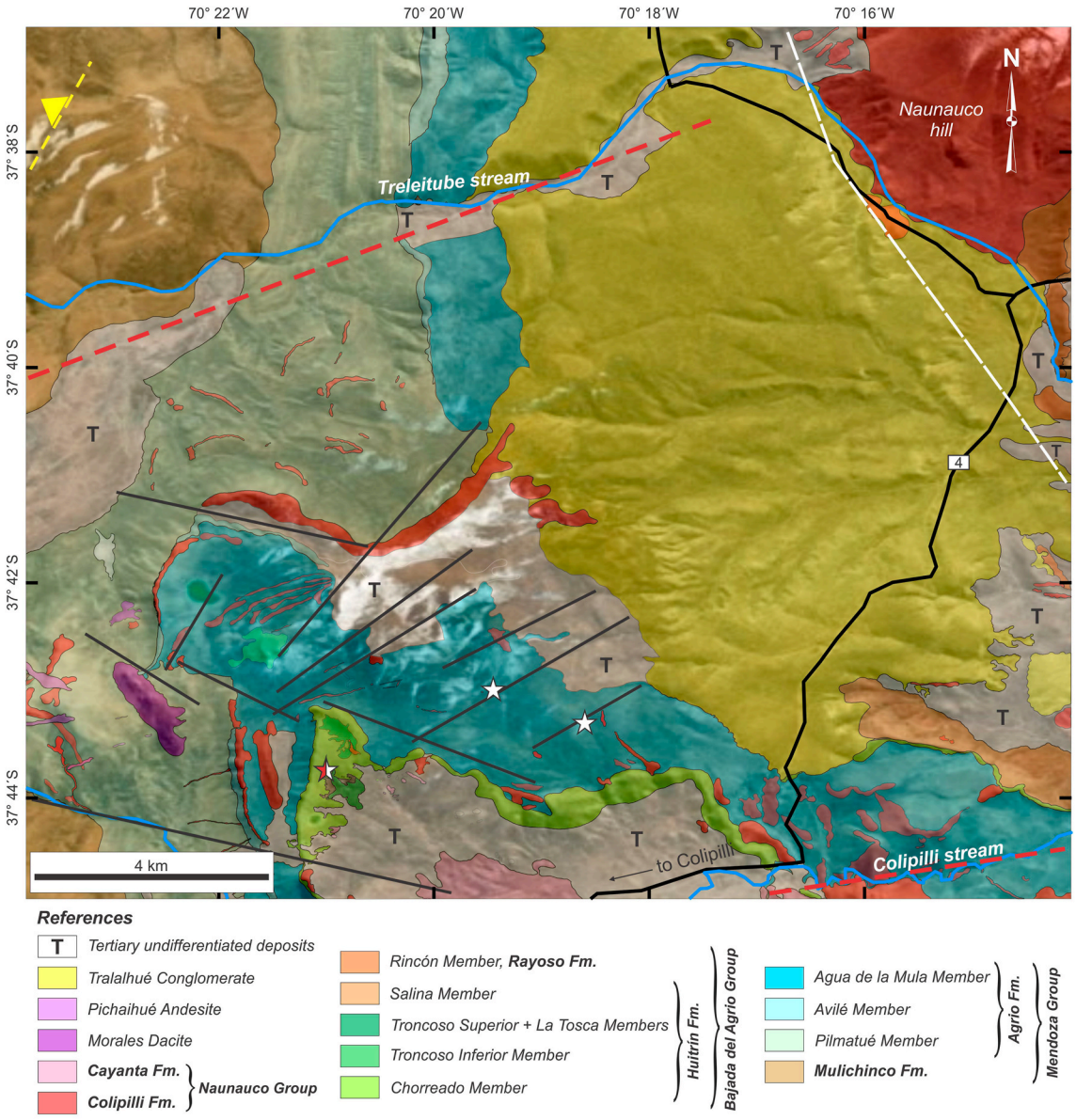

Fig. 2. Satellite image and geological map of the study area and adjacent sectors. White stars indicate vein-type deposits, while the double colored star indicates the presence of bed- and vein-type deposits. **Legends:** red broken lines = pre-Liassic faults; yellow broken lines = pre-Liassic faults reactivated in near orthogonal directions; white broken lines = inner-out deformation limit of the Agrio Fold and Thrust Belt; black lines = shear zones. (For interpretation of the references to color in this figure legend, the reader is referred to the Web version of this article.)

Formation is composed of the Pilmatué, Avilé and Agua de la Mula members, widely distributed on the flanks of anticlines in the study area. The Pilmatué Member is mainly composed of greenish gray to dark gray limestones. The Avilé Member is composed of gray to light brown well-selected medium-grained sandstones. Finally, the Agua de la Mula Member is composed of dark gray pelites interbedded with light brown limestones.

The Bajada del Agrio Group is composed of the Huitrín and Rayoso formations. The first one includes the Chorreado, Troncoso Inferior, Troncoso Superior, La Tosca and Salina members (*e.g.*, Gutiérrez Pleimling, 1991). In the study area, the Chorreado Member is composed of limestones with stylolites and dissolution channels developed on the rock surface. The Troncoso Inferior Member lies above the Chorreado Member through a disconformity and is composed of light brown to whitish fine-grained sandstones with fine lamination and ripples. The Troncoso Superior Member is composed of dark brown limestones with conspicuous lamination, while the La Tosca Member is constituted by light brown dolostones and limestones with a strong fetid smell. Finally, the Salina Member is represented by a few outcrops of varicolored claystones. The Rayoso Formation is composed of reddish sandstones interbedded with reddish limestones.

In addition to the aforementioned stratigraphic units, the occurrence of three petroleum systems was recognized in the area, respectively associated to three source rock sections, namely the Los Molles, Vaca Muerta and Agrio shales (*e.g.*, Cruz et al., 1996; Legarreta et al., 2005, 2008).

The migration of the volcanic arc towards the east during the foreland stage is represented in the study area by intrusive and extrusive intermediate igneous rocks of the Naunauco Group, integrated by the Colipilli and Cayanta formations. The Colipilli Formation includes sills, laccoliths, stocks and dykes. The sills are 1 m thick on average, a few meters long and concordant to the stratification of the Huitrín Formation. The laccoliths are voluminous bodies with slightly vertical development and are commonly emplaced into the Huitrín Formation. The

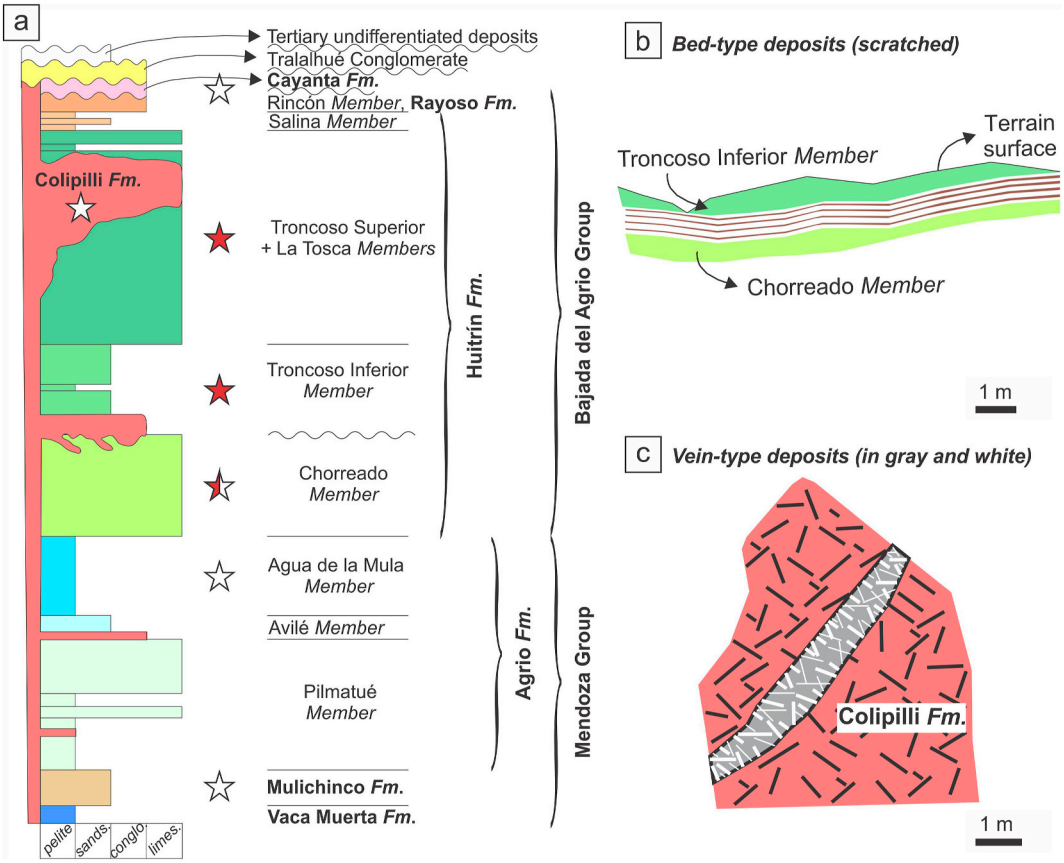

Fig. 3. a) Stratigraphic column of the study area. Red and white stars indicate the presence of bed- and vein-type deposits, respectively, while the double colored star indicates the presence of both types of ore deposits. The wavy line indicates disconformity. **Abbreviations:** sands. = sandstone, conglo. = conglomerate, limes. = limestone. **b, c)** Morphological types of barite-polymetallic deposits and its relationship with the host rocks: concordant to the stratification (b) and crosscutting the stratification (c). (For interpretation of the references to color in this figure legend, the reader is referred to the Web version of this article.)

stocks highlight for their positive topographic expression and crosscut the Vaca Muerta and Mulichinco formations, except in the Naunauco hill where they crosscut the upper part of the Agrio and Huitrín formations. The dykes have 0.8–1.0 m wide and 1.5–3.0 m long and crosscut the entire sedimentary sequence.

In the study area, the barite-polymetallic mineralizations are related to the Early Cretaceous sedimentary sequences and to the Late Cretaceous–Paleocene intrusive bodies. They occur in two main morphological types: beds and veins (Fig. 3). The bed-type deposits have 2.0 m thick on average and are located along the contact between limestones of the Chorreado, Troncoso Inferior and Troncoso Superior members (Huitrín Formation) and the igneous rocks of the Naunauco Group. These deposits are folded and fractured in some sectors. The vein-type deposits have 1.5 m thick on average and are crosscutting the Mulichinco, Agrio and Huitrín formations or the andesitic/dioritic stocks and sills of the Colipilli Formation. These deposits are also fractured in some sectors. The textures of the mineralizations are zebra in the bed-type deposits (Fig. 4a and b) and breccia in the vein-type deposits (Fig. 4c and d).

The stratigraphic succession of the study area culminates with the Tralalhué Conglomerate (Miocene) (Fig. 3). Mass and fluvial removal processes (Quaternary) shaped the current relief of the area.

3. Materials and methods

Petrographic, chemical and microthermometry studies were performed in barite crystals in order to characterize the hydrocarbon-bearing sulphate-polymetallic mineralizations of the Colipilli area. The microthermometry studies were complemented with ultraviolet (UV) incident light and Raman spectroscopy.

Petrographic studies were carried out with a Nikon Optiphot–POL polarized light microscope at the *Instituto de Recursos Minerales* (INREMI, UNLP–CIC). A FEI Quanta 200 scanning electron microscope, equipped with an EDAX SDD Apollo 40 X-ray dispersive energy probe, was also used at the *Laboratorio de Investigaciones de Metalurgia Física* (LIMF, UNLP).

Electron microprobe analyses were performed with JEOL Superprobe JXA-8230 microprobes at the *Serveis Científics i Tecnòlogics* (SCiT; *Universitat de Barcelona*, Spain) and the *Laboratorio de Microscopía Electrónica y Análisis por Rayos X* (LAMARX; *Universidad Nacional de Córdoba*, Argentina). A CAMECA Camebax SX-100 microprobe of the Geology Department of the *Universidad de Oviedo* (Spain) was also used. The barite crystals were analyzed using a current acceleration of 15 kV, an electric current between 10 and 20 nA and a beam diameter of 1–2 μm. Calibrations were performed using natural and synthetic standards. Longitudinal and transversal profiles to the crystal elongation were made in order to determine possible zonal compositional variations. End-member proportions were calculated based on the obtained results following the method of Deer et al. (1992).

In order to determine the presence of hydrocarbons and to avoid the introduction of errors by heating, fluorescence techniques with incident UV light and Raman spectroscopy were carried out before the microthermometry measurements. The UV incident fluorescence analysis was performed at the *Universidad Nacional del Sur*, Argentina, with a Nikon Eclipse 50iPOL microscope. A 100 W mercury-vapor lamp with filters for UV (λ = 334–365 nm), blue (λ = 435–490 nm) and green (λ = 546 nm) irradiation bands was used as light source. This method allows to quickly distinguish non-fluorescent aqueous inclusions from those with

Fig. 4. Photographs of the bed- (**a, b**) and vein-type (**c, d**) deposits of the Colipilli area. The black oval in figure "a" indicates a hammer placed to show the scale.

fluorescent hydrocarbons (Burrus, 1981). The Raman spectra were obtained at the Laboratory of Microscopy and Raman Spectroscopy of *YPF Tecnología* (Y-TEC), Argentina, with an NRS-4100 Jasco spectrometer equipped with a 532 nm laser and a set of holographic filters, coupled to an Olympus microscope. This technique allows the gaseous composition inside the inclusion to be determined (*e.g.*, CH_4, CO_2).

The fluid inclusions (FI) microthermometry studies were performed at the INREMI and the *Universidad Nacional del Sur* with Linkam MDS 600 heating-cooling plates mounted on Olympus BX50 microscopes. These plates allow heating up to 600 °C and cooling up to −196 °C. FI studies were performed in order to obtain physicochemical data of the hydrothermal system in which the mineralization was formed: temperature, general composition of the fluid phase and possible interaction between fluids of different origins (inorganic *vs.* organic).

4. Description of the barite-polymetallic mineralizations

A set of barite-polymetallic mineralizations occur in the Colipilli area in two main morphological types: a) bed-type deposits, concordant to the stratification (Fig. 3b), and b) vein-type deposits, crosscutting the stratification (Fig. 3c).

4.1. Bed-type deposits

Bed-type deposits are emplaced along the contact between the igneous rocks of the Naunauco Group and their sedimentary host rocks, especially the Huitrín Formation. Additionally, these deposits are emplaced in sedimentary host rocks as the Chorreado Member mudstones, the Troncoso Inferior Member fine-grained sandstones and/or the Troncoso Superior Member laminated limestones (Fig. 4a and b). The bed-type deposits have NE-SW direction, dip 30–55° towards the SE and are up to 6.0 m long and 1.5 m wide. They are composed of microgranular barite with minor contents of Fe-oxyhydroxides, galena and pyrite. Mantiform levels of magnetite also appear within the fine carbonate horizons of the Chorreado Member.

The bed-type deposits have zebra texture characterized by a rhythmic alternation of white and dark brown bands (Fig. 5a and b). This texture is present in most of the limestones of the Troncoso Superior and Chorreado members. The white bands have an average thickness of 0.2 cm and are mainly composed of microgranular and tabular barite up to 0.5 cm in length (Fig. 5a). Barite crystals frequently have a radial arrangement and dissolution structures with dispersed pyrite of millimeter size. In some sectors, calcite is replaced by small barite crystals. The dark brown bands have an average thickness of 0.3 cm and are mainly composed of calcite (Fig. 5a). This banding is interrupted by small displacements of 0.3 cm in length (Fig. 5b). A sulfide mineralization overlaps the zebra texture and consists of well-developed galena crystals 1 cm in average size, which is strongly replaced by cerussite and accompanied by minor amounts of cubic-shaped and millimeter-sized pyrite crystals. Limestones are recrystallized and impregnated with Fe-oxyhydroxides, while the igneous rocks are kaolinitized.

On the other hand, barite hosted in the fine-grained whitish laminated sandstones of the Troncoso Inferior Member consists of microgranular and tabular crystals up to 0.8 cm in length. Barite forms thin bands from few millimeters to 1.5 cm thick that are interdigitated with the sandstone lamination planes. Galena crystals with an average diameter of 1 cm overlap with those of barite. In addition, millimeter-sized pyrite boxworks associated with galena were also identified.

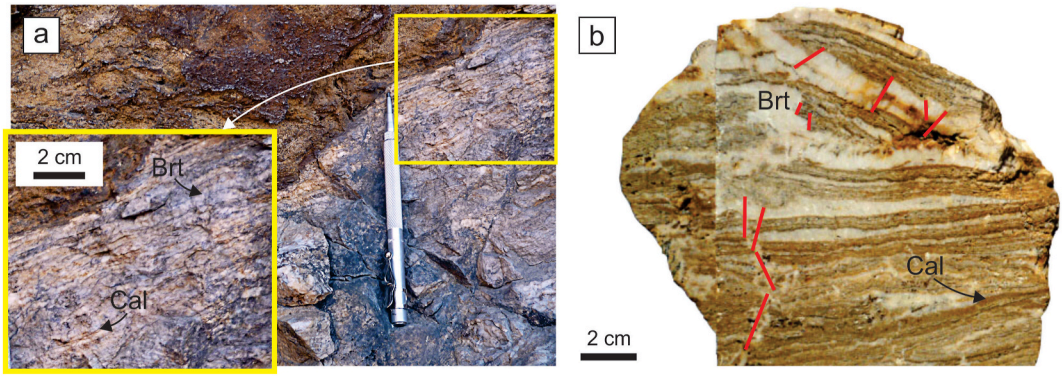

Fig. 5. a) Outcrop-scale zebra texture (pencil length = 13 cm). The yellow square is a detail of the zebra texture. **b)** Polished hand sample with small vertical displacements. **Abbreviations:** Brt = barite, Cal = calcite. (For interpretation of the references to color in this figure legend, the reader is referred to the Web version of this article.)

4.2. Vein-type deposits

Vein-type deposits are crosscutting the sedimentites of the Mulichinco, Agrio and Huitrín formations and the andesitic/dioritic stocks and sills of the Colipilli Formation. The contact between the veins and their host rocks is clear and straight. The vein-type deposits have N–S direction, dip 70–80° towards the E and are 1.5 m thick on average. They are composed of spatic barite with minor amounts of Fe-oxyhydroxides (Fig. 4c and d) and sulfides (galena > chalcopyrite > pyrite > sphalerite > tetrahedrite).

The vein-type deposits commonly have breccia texture characterized by sub-angular clasts of spatic barite and laminated limestone cemented by microgranular barite crystals and Fe-oxyhydroxides. The veins sometimes present a banded structure determined by a random arrangement of barite crystals located in the central portion and Fe-oxyhydroxides at both sides (Fig. 6a). Barite also forms irregular groups of crystals with great variability in their grain size, from few centimeters to 10 cm in length. These aggregates of barite crystals are sometimes fractured and flexed (Fig. 6b). In some places, rosette and comb textures can be observed (Fig. 6c and d). Galena is scarce and has cubic habit (although some grains are anhedral) with a maximum size of 1 cm. Chalcopyrite is recognized as patinas with aggregates of 2–3 cm in size. Pyrite is found dispersed, exceptionally fresh and in most cases oxidized to limonite. Frequently, cubic cavities of millimeter size generated by leaching processes can be observed. The supergenic minerals such as malachite, azurite, cerussite, calcosina, covelina and Fe-oxyhydroxides overlap the primary paragenesis, giving the whole rock a reddish, greenish and/or dark gray coloration. Igneous host rocks show discoloration caused by sericitization and are impregnated with Fe-oxyhydroxides.

4.3. Petrography

Barite crystals from bed-type deposits are developed in the original carbonate matrix and show variable habits, such as fibrous, prismatic or tabular, in some cases forming radial aggregates (Fig. 7a and b). Some

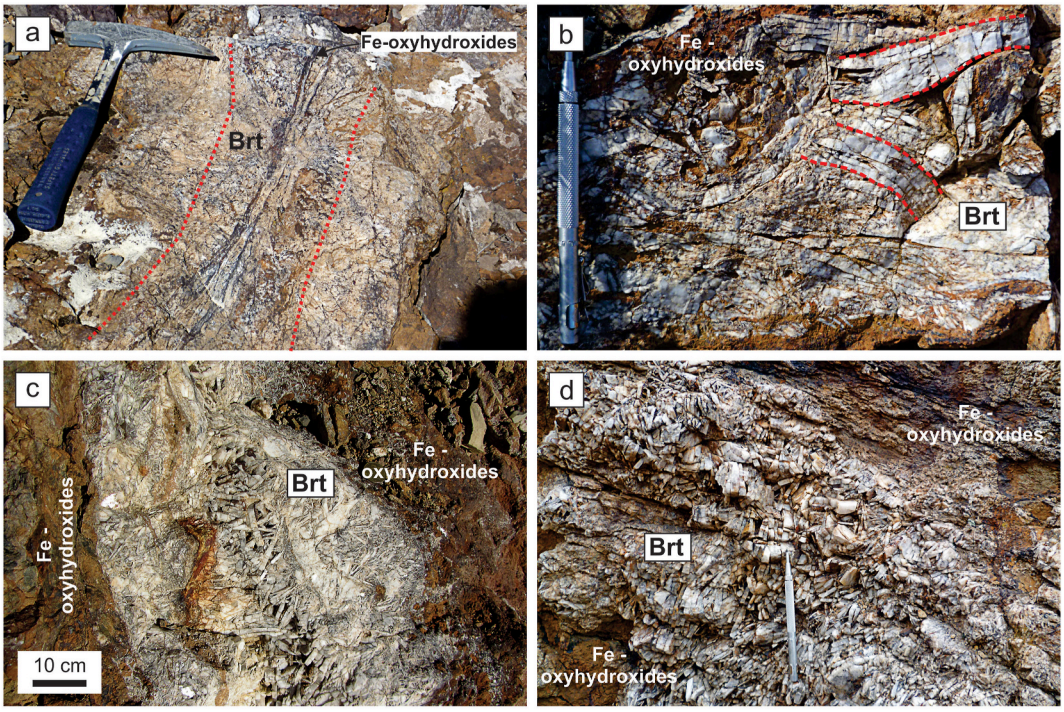

Fig. 6. a) Vein-type deposit with banded appearance. **b)** Flexed and fractured barite (Brt) crystals with tabular habit. **c, d)** Barite crystals with tabular habit grouped forming comb and radiated structures. The pencil in figures "b" and "d" was placed to show the scale (pencil length = 13 cm).

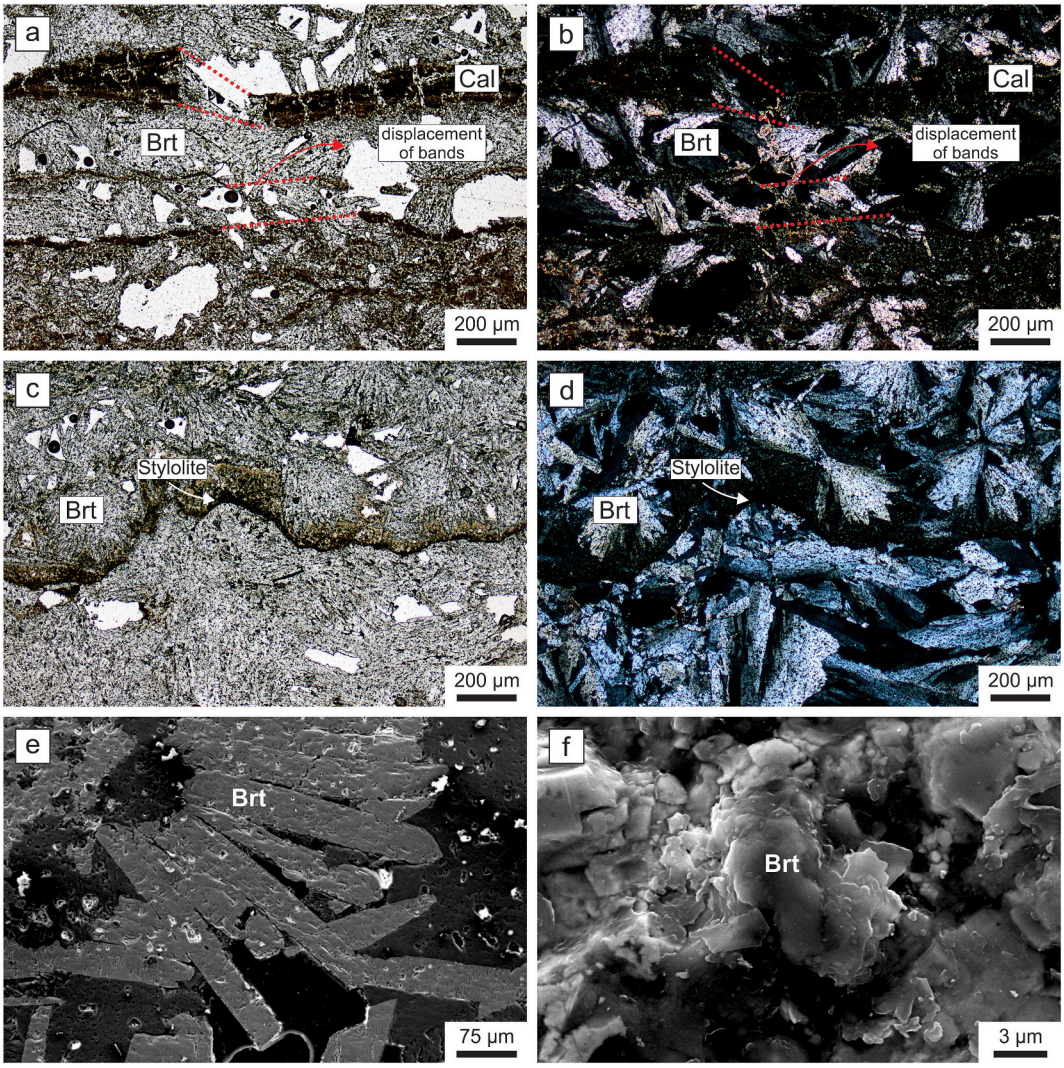

Fig. 7. a, b) Barite crystals with radiated growth and small displacements (a: plane polarized light view; b: crossed Nicols view). **c, d)** Barite crystals with bipolar growth and stylolites (c: plane polarized light view; d: crossed Nicols view). **e, f)** Scanning electron microscope images of barite crystals with pyramidal morphologies at their ends (e) and radiated growth (f). **Abbreviations:** Brt = barite, Cal = calcite.

prismatic crystals exhibit pyramidal morphologies, while others exhibit bipolar growth (Fig. 7c and d). In the back-scattered electron images, barite crystals show tabular morphologies (Fig. 7e) with layer-by-layer growth of the mineral (Fig. 7f). These crystals are 300–600 µm long and 50–100 µm wide. Galena crystals are subhedral and up to 0.8 mm in size; their borders are replaced by cerussite. In some galena crystals, very small pyrite inclusions (0.4 mm) replaced by limonite can be observed.

Barite crystals from vein-type deposits are randomly distributed, show prismatic and tabular habits and form radial aggregates (Fig. 8a and b). In the back-scattered electron images, barite crystals exhibit thick tabular habits and rosette-like structures (Fig. 8c). Many crystals are fractured and flexed and show evidence of dissolution (Fig. 8d). The smallest crystals are 335 µm long and 45 µm wide, while the largest crystals are 3 mm long and 635 µm wide. Galena crystals are subhedral and euhedral and have an average size of 0.1 cm; in some cases, cerussite is observed replacing galena contours. Chalcopyrite is recognized as xenomorphic masses of 0.7 mm in size, sometimes incipiently replaced by calcosina and covelina. Small cubic pyrite crystals (up to 0.5 mm) are shown scattered and partially replaced by limonite. Sphalerite and tetrahedrite were identified as small inclusions (0.2 mm on average) hosted in xenomorphic chalcopyrite masses and galena crystals.

5. Barite chemical composition

Table 1 shows the compositional variations between barites from bed- and vein-type deposits, including the means and standard deviations, as well as the molecular proportions of the final components. Barite from bed-type deposits has BaO, SrO and SO_3 contents of 61.74–65.46 wt %, 0.11–3.60 wt % and 31.69–35.41 wt %, respectively; the CaO content reaches 0.11 wt %. On the other hand, barite from vein-type deposits has BaO and SO_3 contents of 63.38–67.45 wt % and 31.99–34.79 wt %, respectively; the SrO and CaO contents reaches 2.00 wt % and 0.08 wt %, respectively. These values are congruent with barites defined by the classification of Burkhard (1978).

The ternary diagram of the barite-celestine-anhydrite series ($BaSO_4$–$SrSO_4$–$CaSO_4$; Bolonin and Nikiforov, 2014) is shown in Fig. 9. It should be noted that the studied barites are concentrated around the $BaSO_4$ vertex of the diagram, reflecting a compositional homogeneity and very low Sr contents. It can also be observed that the Sr content is lower in vein-type deposits than in bed-type deposits. For comparative purposes, Fig. 9 also includes the sulphate compositions of other deposits of the Neuquén Basin (de Barrio et al., 2016), which reflect the existence of three groups: two around the $BaSO_4$ and $SrSO_4$ vertices and an intermediate group. It should also be noted that within each deposit there is a tendency for bed-type deposits to have a higher degree of

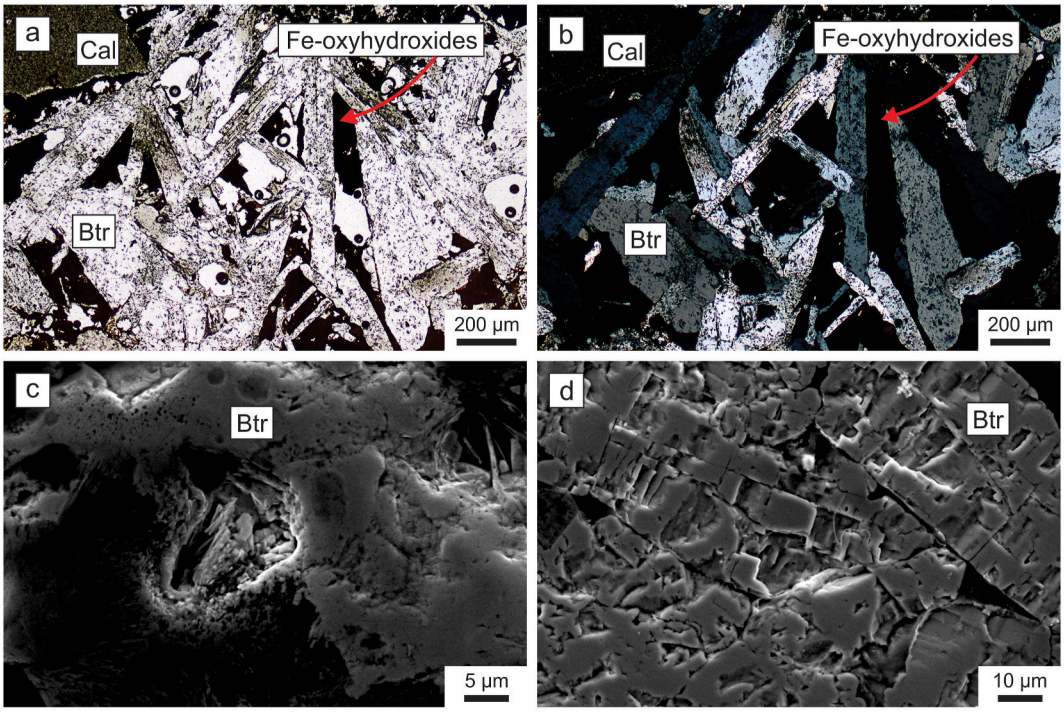

Fig. 8. a, b) Barite crystals with prismatic to thick tabular habit with random arrangement (a: plane polarized light view; b: crossed Nicols view). **c, d)** Scanning electron microscope images of barite crystals with thick tabular habit, rosette-like structures (c) and intense degree of fracturing (d). **Abbreviations:** Brt = barite, Cal = calcite.

Ba–Sr mixture.

6. Fluid inclusion studies

6.1. Petrography of fluid inclusions with transmitted and UV light

Fluid inclusions (FI) in barite from bed- and vein-type deposits were classified according to their genesis, number of phases, relief and size and color of the bubble (Roedder, 1963). In addition, other observations were made due to the possible presence of hydrocarbons, following the criteria of Burrus (1981): 1) hydrocarbon presence in FI may be indicated by yellow, brown and/or black bubbles, 2) hydrocarbons have refractive indexes close to those of host minerals, 3) hydrocarbon presence may be indicated by behavior changes of phases during freezing (see also Roedder, 1963), and 4) FI containing aromatic hydrocarbons fluoresce under UV light.

The FI were first classified as primary and secondary considering its genesis (Fig. 10). They were also classified as Type I (one phase, generally liquid), Type II (liquid + gas) and Type III (liquid + gas + solid) according to the number of recognized phases (Table 2) (Goldstein and Reynolds, 1994). The bubbles of the different types of FI are between 20 and 40 μm in size. Type I corresponds to a group of FI with subhedral habit and normal relief. Type II is represented by four families of FI with mainly colorless bubbles. The first family (Type IIa) has anhedral habit and a liquid phase with very low refractive index, similar to barite (1.63–1.64). The second family (Type IIb) has anhedral habit and moderate relief. The third family (Type IIc) has euhedral habit. Finally, the fourth family (Type IId) has anhedral habit, moderate to high relief, colorless liquid phase and colorless to pink bubbles. Type III corresponds to a group of FI with subhedral habit, normal relief and colorless solid phases with tabular prismatic habit inclusions. The characteristics of bubbles in the latter type allow to differentiate it into two families: one with high relief and pinkish bubbles (Type IIIa) and another with low relief and colorless bubbles (Type IIIb).

The UV light fluorescence study allowed FI to be classified into two large sets: fluorescent (types IId and IIIa) and non-fluorescent (the remaining types of FI) (Fig. 11). The fluorescent set of FI have bluish hues.

6.2. Fluid inclusions Raman spectroscopy

Raman spectroscopy studies confirmed the aqueous composition of the non-fluorescent set of FI and the presence of liquid hydrocarbons in the highly fluorescent set of FI (types IId and IIIa). However, clear discrimination of the characteristic peaks was not possible, since the spectra is strongly affected by the fluorescence phenomenon (Fig. 12). The elevated fluorescence, such as that emitted by hydrocarbons containing cyclic or aromatic groups (Burke, 2001), is a limitation of the technique. The latter is due to the elevated fluorescence which is several orders of magnitude greater with respect to the Raman signals and, consequently, masks them.

6.3. Fluid inclusions microthermometry

The microthermometry studies were carried out only on primary FI (types II and III without hydrocarbons) because its content corresponds to the fluid trapped during the mineral crystallization and represents a small sample of the original fluid. Only a few of the numerous Type II FI were measured. The small size and high hydrocarbon content of most of them made measurements impossible. It should be noted that high hydrocarbon contents give erroneous results. In all heating measurements, the homogenization temperature (T_h) was considered meaningful only in aqueous FI without evidence of hydrocarbons. Those FI where an irreversible bubble increase was observed during heating were suspected of containing hydrocarbons. This could be caused by cracking of liquid organic components that became part of the gas phase. These measurements were discarded. Additionally, FI with leaks, necks or decrepitations were also discarded to avoid results representative of post-entrapment processes (Goldstein and Reynolds, 1994).

Minimum entrapment temperatures were estimated from the T_h of

Table 1
Electron microprobe analyses of barite crystals from the Colipilli area (Neuquén Basin, Argentina).

	Bed-type deposits						Vein-type deposits					
Location	37° 43′ 39″ S; 70° 20′ 53″ W						37° 43′ 55″ S	70° 20′ 45″ W	37° 43′ 02″ S	70° 18′ 25″ W	37° 43′ 40″ S	70° 20′ 57″ W
Sample	11227a (n = 16)		11227b (n = 11)		19407 (n = 28)		4951 (n = 12)		21847 (n = 57)		19373 (n = 35)	
wt. %	Mean	Std	Mean	std	Mean	std	Mean	std	Mean	std	Mean	std
FeO_T	0.0073	0.0093	0.0190	0.0261	0.0000	0.0000	0.0000	0.0000	0.0115	0.0199	0.0922	0.2314
MnO	0.0002	0.0008	0.0000	0.0000	0.0000	0.0000	0.0000	0.0000	0.0235	0.0238	0.0321	0.0285
CoO	0.0000	0.0000	0.0000	0.0000	0.0229	0.0163	0.0177	0.0205	0.0068	0.0149	0.0210	0.0323
MgO	0.0084	0.0079	0.0069	0.0089	0.0000	0.0000	0.0013	0.0020	0.0064	0.0107	0.0052	0.0079
CaO	0.0340	0.0288	0.0255	0.0146	0.0146	0.0177	0.0109	0.0156	0.0153	0.0135	0.0059	0.0146
SrO	1.4869	0.6826	1.6071	0.8325	1.1389	0.6996	1.0348	0.6107	2.0788	0.4254	0.5728	0.4468
BaO	64.1680	0.7339	64.0963	1.0485	64.5014	0.9550	64.6304	0.9731	63.7340	1.0632	65.4291	0.9481
P_2O_5	0.0005	0.0015	0.0183	0.0335	0.0000	0.0000	0.0000	0.0000	0.0000	0.0000	0.0000	0.0000
PbO	0.0118	0.0473	0.0069	0.0229	0.0425	0.0660	0.0000	0.0000	0.0000	0.0000	0.0005	0.0023
SO_3	33.8709	0.9192	34.3240	0.5658	33.8839	0.7972	34.0153	0.7675	34.2186	0.5987	33.5494	0.3681
F	0.0022	0.0045	0.0034	0.0035	0.0000	0.0000	0.0000	0.0000	0.0000	0.0000	0.0000	0.0000
Total	**99.5903**	–	**100.1074**	–	**99.6043**	–	**99.7103**	–	**100.0950**	–	**99.7084**	–
Ions calculated on the basis of 4 oxygens per formula unit												
Sample	11227a (n = 16)		11227b (n = 11)		19407 (n = 28)		4951 (n = 12)		21847 (n = 57)		19373 (n = 35)	
c.p.f.u.	**Mean**	**std**	**Mean**	**std**	**Mean**	**std**	**Mean**	**std**	**Mean**	**std**	**Mean**	**std**
Fe^{2+}	0.0002	0.0003	0.0006	0.0008	0.0000	0.0000	0.0000	0.0000	0.0004	0.0006	0.0029	0.0072
Mn	0.0000	0.0000	0.0000	0.0000	0.0000	0.0000	0.0000	0.0000	0.0008	0.0008	0.0010	0.0009
Co	0.0000	0.0000	0.0000	0.0000	0.0007	0.0005	0.0005	0.0006	0.0002	0.0004	0.0006	0.0010
Mg	0.0005	0.0005	0.0004	0.0005	0.0000	0.0000	0.0001	0.0001	0.0004	0.0006	0.0003	0.0005
Ca	0.0014	0.0012	0.0010	0.0006	0.0006	0.0007	0.0004	0.0006	0.0006	0.0006	0.0002	0.0006
Sr	0.0330	0.0150	0.0356	0.0183	0.0254	0.0156	0.0231	0.0136	0.0459	0.0093	0.0127	0.0099
Ba	0.9647	0.0148	0.9608	0.0169	0.9729	0.0154	0.9759	0.0136	0.9518	0.0095	0.9821	0.0112
P	0.0000	0.0000	0.0006	0.0011	0.0000	0.0000	0.0000	0.0000	0.0000	0.0000	0.0000	0.0000
Pb	0.0001	0.0005	0.0001	0.0002	0.0004	0.0007	0.0000	0.0000	0.0000	0.0000	0.0000	0.0000
Sum	**1.0000**	–	**0.9991**	–	**1.0000**	–	**1.0000**	–	**1.0000**	–	**1.0000**	–
S	0.9935	0.0086	0.9962	0.0046	0.9945	0.0057	0.9957	0.0075	0.9945	0.0071	0.9908	0.0046
Total	**1.9935**	–	**1.9953**	–	**1.9945**	–	**1.9957**	–	**1.9945**	–	**1.9908**	–
End-members proportions												
Anhydrite	0.14	0.12	0.10	0.06	0.06	0.07	0.04	0.06	0.06	0.06	0.02	0.06
Celestite	3.30	1.50	3.57	1.83	2.54	1.56	2.31	1.36	4.60	0.94	1.28	1.00
Barite	96.56	1.52	96.33	1.86	97.40	1.56	97.65	1.38	95.34	0.93	98.70	0.99
Total	**100.00**	–	**100.00**	–	**100.00**	–	**100.00**	–	**100.00**	–	**100.00**	–

the aqueous FI (Roedder, 1984). Since the analyzed system was developed under superficial conditions, the pressure was not considered as an important factor in the modification of the temperature. Therefore, the T_h has been considered as the real entrapment temperature. Fluid salinity was obtained from the final ice melting temperature (T_{fm}) using the tables of Goldstein and Reynolds (1994); these values are expressed in wt. % NaCl equivalent. Given the small size of the inclusions and the turbidity of the barite crystals, the initial ice melting temperature (T_{im}), also known as eutectic temperature, was rarely observed and the composition of the fluid phase could not always be determined. Table 3 summarizes the obtained results.

The bubbles of the two-phase FI from bed-type deposits normally disappeared during cooling. During system temperature recovery, it was possible to determine initial ice melting temperatures (T_{im}) between −44.0 and −21.1 °C. These temperatures correspond to the following systems: NaCl–H_2O (−21.2 °C), NaCl–$MgCl_2$–H_2O (−55.0 to −37.0 °C; metastable) and NaCl–KCl–H_2O (−28.0 °C; metastable). The final ice melting temperature (T_{fm}) were observed between −4.5 and −0.1 °C, indicating salinities between 0.18 and 7.17 wt % NaCl equivalent. During the heating processes, many bubbles showed Brownian movement and homogenized to liquid at T_h between 156.2 and 176.0 °C.

As in the previous case, the bubbles of the two-phase FI from vein-type deposits normally disappeared during cooling. During system temperature recovery, it was possible to determine T_{im} between −52.0 and −23.3 °C. These temperatures correspond to the same chemical systems determined for the FI of the bed-type deposits, suggesting the presence of one or more dissolved salts in the fluid phase. The observed T_{fm} varies between −5.3 and −0.3 °C, indicating salinities between 0.53 and 8.28 wt % NaCl equivalent. During the heating processes, the bubbles showed Brownian movement and homogenized to liquid at T_h between 223.0 and 280.6 °C.

7. Discussion

The bed- and vein-type deposits of the Colipilli area consist of barite mineralizations with overlapped Fe-oxyhydroxides and sulfides. The bed-type deposits are emplaced along the contact between limestones and sandstones of the Huitrín Formation (Chorreado, Troncoso Inferior and Troncoso Superior members) and the intrusive and extrusive intermediate igneous rocks of the Naunauco Group. In contrast, the vein-type deposits are crosscutting the Mulichinco, Agrio and Huitrín formations or the andesitic/dioritic stocks and sills of the Naunauco Group. The bed- and vein-type deposits are characterized by the presence of zebra and breccia textures, respectively. The main characteristics of the barite-polymetallic deposits of the Colipilli area are summarized in Table 4.

The zebra texture revealed that the rhythmic alternation of white and dark brown bands is a consequence of the preferential replacement of calcite by barite as suggested by Llambías and Malvicini (1978). Vertical displacements and folding of these deposits evidence the effects of compressive tectonic efforts occurred in the region. In dolostones of the southern Brabant-Wales Massif, Belgium, small vertical displacements of the bands, such as those described for the Colipilli area, were also observed by Nielsen et al. (1998), who defined them as a typical feature of the zebra texture. Likewise, Vanderginste et al. (2005) recognized similar features in the carbonate rocks of the Rocky

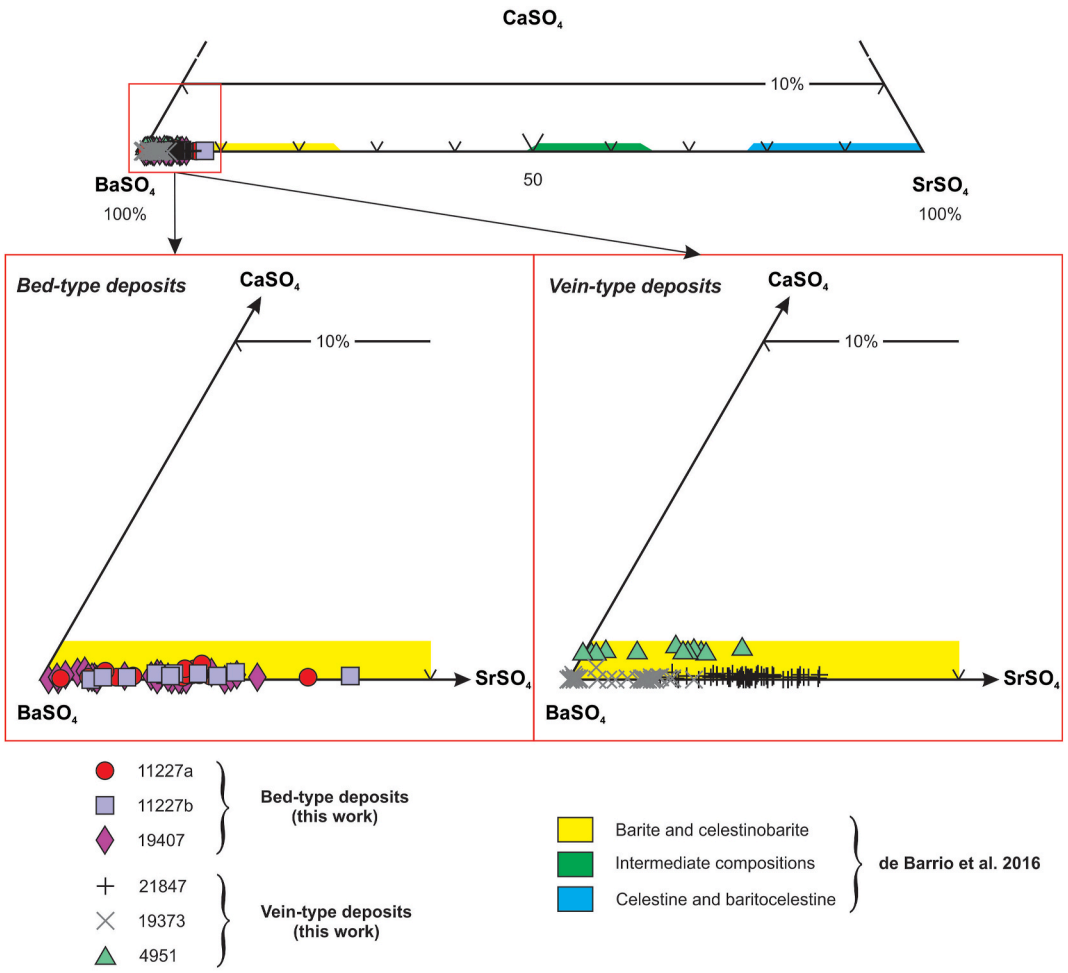

Fig. 9. Ternary diagram of the barite-celestine-anhydrite series ($BaSO_4$–$SrSO_4$–$CaSO_4$; based on Bolonin and Nikiforov (2014)) for barites investigated in this work together with sulphate compositions published by de Barrio et al. (2016) for other Ba–Sr deposits of the Neuquén Basin.

Mountains Fold and Thrust Belt, Canada, and linked them to regional compressive tectonic efforts.

The breccia texture points out the action of successive mineralizing filling pulses. Brodtkorb et al. (1975) proposed a syngenetic origin for this texture. According to these authors, descending solutions dissolved the banks of evaporitic sulphates and reprecipitated them at lower stratigraphic levels. Alternatively, Hayase and Bengochea (1975) proposed an epigenetic (hydrothermal) origin for this texture, based on the analysis of nine barite occurrences. This last hypothesis was also supported by Llambías and Malvicini (1978), Collao et al. (1997), Collao (1998) and de Barrio et al. (2009, 2014).

The mineralogical and textural characteristics recognized in the barite-polymetallic mineralizations of the Colipilli area indicate an epigenetic origin. In this sense, Llambías and Malvicini (1978) had already defined the bed- and vein-type deposits of the Colipilli area as replacement and filler products of the carbonate levels.

The presence of barite crystals with high degree of crystallinity and bipolar growth indicate that the mineralizing fluids preferentially circulated through weakness zones, such as the marked lamination and dissolution structures of limestones and the discordance surface existing between the Chorreado and Troncoso Superior members (Huitrín Formation). Furthermore, de Barrio et al. (2009) and Escobar et al. (2013a, b) proposed that a favorable level for the migration of mineralizing fluids would be represented by a porous and permeable horizon, limited at its base by an impermeable layer that constitutes a lithostratigraphic control. In the Colipilli area, the permeable layer could be represented by the laminated limestones of the Chorreado and Troncoso Superior members and the fine-grained sandstones of the Troncoso Inferior Member (Huitrín Formation). On the other hand, the impermeable level of the study area could be represented by the cuspidal pelitic horizon of the Agua de la Mula Member (Agrio Formation), which limited and controlled the development of the mineralization.

The study of fluid inclusions (FI) hosted in barite crystals from bed- and vein-type deposits revealed different types (I, II and III) and families of primary FI. The fluorescence observed with UV incident light allowed FI that range from completely aqueous to completely organic, including all the intermediate terms, to be identified. Moreover, the Raman spectroscopy results confirmed that FI with strong fluorescence contain liquid hydrocarbons. The microthermometry studies carried out only on the aqueous FI, allowed the conditions of formation of the barite deposits to be determined. Vein-type deposits formed at higher temperatures and slightly higher salinities (T_h = 249.7 °C on average; 0.5–9.3 wt % NaCl equivalent) than bed-type deposits (T_h = 162.2 °C on average; 0.2–7.2 wt % NaCl equivalent).

Regarding the organic FI, the sulphate-dissolved hydrocarbon association is thermodynamically unstable in all diagenetic environments. Thus, sulphate is susceptible to be reduced either organically (bacterial sulphate reduction, BSR) or inorganically (thermochemical sulphate reduction, TSR) (Machel, 1998). The BSR is considered the most important process in the sulfide formation. It is common between 0 and 60–80 °C; above this temperature range, almost all sulphate-reducing bacteria stop metabolizing (Machel, 1998). In addition to a sulphate source, the BSR requires the presence of a reducing environment that enables the development of sulphate-reducing bacteria (Seal II, 2006).

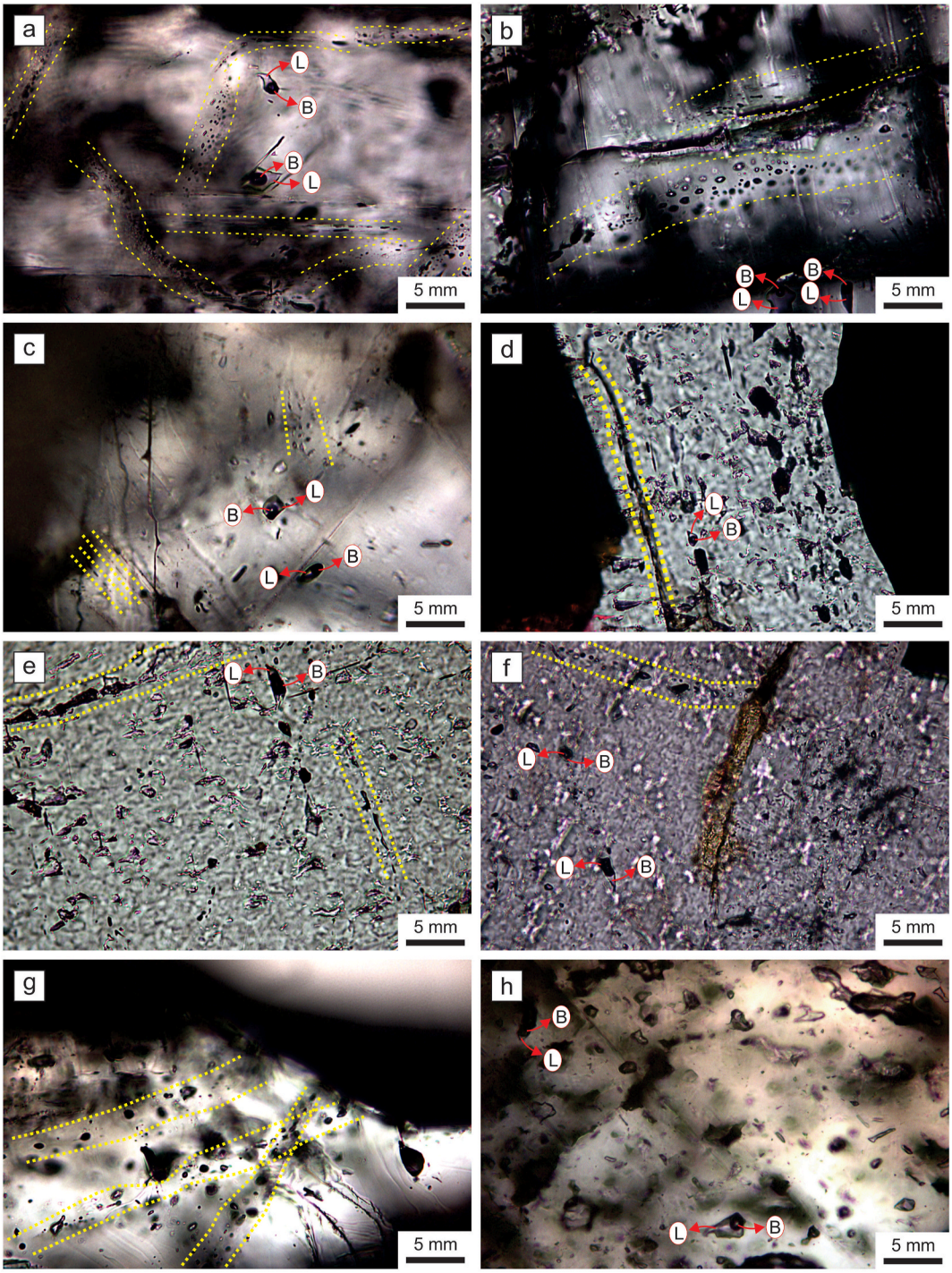

Fig. 10. a-g) Primary FI and "trends" of secondary FI associated with small fractures in barite crystals from bed-type deposits. The "trends" of secondary FI are indicated with yellow broken lines. **h)** Primary FI in barite crystal from vein-type deposits. **Abbreviations:** B = bubble, L = liquid. (For interpretation of the references to color in this figure legend, the reader is referred to the Web version of this article.)

In presence of organic matter, the TSR is another process that produces large amounts of H_2S. The temperature range in which this process works is between 100 and 140 °C, although there are records of higher temperatures than 160–180 °C (Machel, 1998). The most common sulfides that are formed by the TSR process are galena, sphalerite and minor amounts of pyrite.

The presence of hydrocarbons in FI from the Colipilli area could be responsible for the reducing environment (Salvioli, 2017). This context generates the best conditions for galena, chalcopyrite, pyrite, sphalerite and tetrahedrite formation, among other sulfides, depending on the availability of metals in the system. The temperatures determined for the Colipilli barite deposits suggest that the TSR process was responsible for the reducing conditions that led to the formation of sulfides. The TSR process was observed by Alberdi-Genolet et al. (2013) in an atypical petroleum system developed in Valle del Río Grande, in the northern portion of the Neuquén Basin, related to a Miocene magmatism that intruded source rocks of the Mendoza Group. A petroleum system is considered atypical when the hydrocarbon generation processes are different from those of maturation by burial, such as the thermal effect of igneous intrusions in source rocks (Magoon and Dow, 1994).

Table 2
Types of fluid inclusions identified in barite crystals from the Colipilli area (Neuquén Basin, Argentina).

Type of fluid inclusion	Family	Morphology	Fluorescence	Composition
I	–		No	Aqueous
II	a		No	Aqueous
	b		No	Aqueous
	c		No	Aqueous
	d		Yes	Hydrocarbons
III	a		Yes	Hydrocarbons
	b		No	Aqueous

In addition to the recognition of organic fluids in the bed- and vein-type deposits, it was possible to estimate the composition of the hydrocarbons based on its fluorescence color (bluish hues). Numerous authors have correlated fluorescence colors with the API gravity coefficient (*e.g.*, Bodnar, 1990; Tsui, 1990; Stasiuk and Snowdon, 1997). The increase in the wavelength of the fluorescent emission corresponds to a decrease in the API degrees of the hydrocarbons. Thus, green, orange and reddish fluorescence colors correspond to lower API values than for emissions with different hues of blue (Fig. 13) (Riecker, 1962). The strong fluorescence in bluish hues, presented by our Type IId and Type IIIb families of FI, show a hydrocarbon of advanced maturity (light) with medium to high API gravity (*ca.* 40°). These values are correlated with the window for the generation of liquid/gaseous hydrocarbons. This degree of hydrocarbon maturity is in accordance with that determined by Legarreta et al. (2008) for the Puesto Rojas-El Portón district, within which the Colipilli area is included.

7.1. Evolutionary model of the mineralizing fluids for the Colipilli barite deposits

The characteristics of barites from the Colipilli area are the consequence of its complex genesis, which involved the interaction of fluids with different origins. In this sense, processes like rock replacement and fracture filling were associated with the circulation of hydrothermal fluids of inorganic and organic nature of different compositions and temperatures.

Llambías and Malvicini (1978) proposed that the Late Cretaceous–Paleocene magmatism of the Naunauco Group would have provided the necessary heat to cause the movement of magmatic, connate and meteoric waters. During the emplacement and crystallization of intrusive rocks of the Colipilli Formation, the increase in temperature of the host rocks was probably followed by the influx of magmatic waters that were mixed with connate waters. The latter come from the dehydration caused by heating and compaction generated by the weight of the Lower Cretaceous sedimentary pile above the deepest stratigraphic levels. Furthermore, the migration of hydrothermal fluids was favored by the primary and secondary porosity of the involved rocks (Agirrezabala et al., 2014; Senger et al., 2017).

The association between dissolved sulphates and hydrocarbons is thermodynamically unstable (Machel, 2001). As a result of this instability, redox reactions reduced the sulphate generating H_2S, HS^-, HCO_3^- and CO_2. The production of these volatiles implies a large volumetric expansion of the fluid phase (Dubessy and Ramboz, 1986), increasing the fluid pressure and, consequently, causing hydraulic fracturing of the host rocks. The latter process could be related to the breccia texture development in the vein-type deposits hosted in the Mulichinco and Agrio formations. Overpressure processes like this have also been described in other hydrothermal systems generated by igneous intrusions into hydrocarbon source rocks (*e.g.*, Rodríguez Monreal et al., 2009; Cobbold et al., 2014; Spacapan et al., 2020).

The mobilization of fluids promoted the leaching of metallic and non-metallic elements (mainly Ba and Sr and minor amounts of Fe, Pb, Cu and Zn) from the highly reactive sedimentary sequence (Fig. 14).

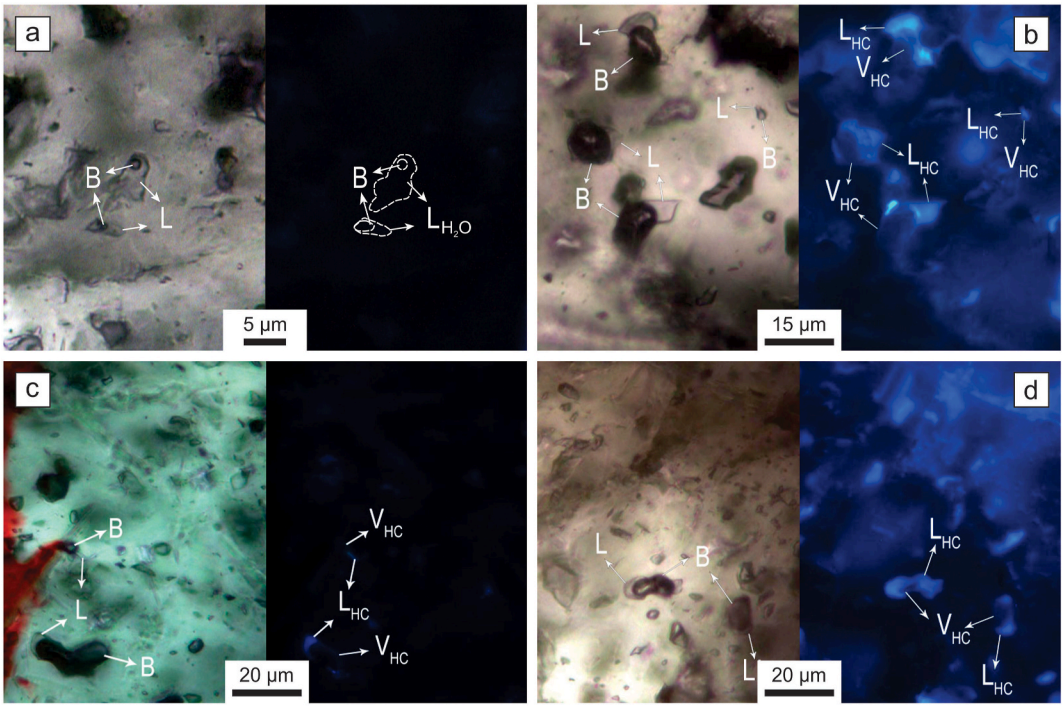

Fig. 11. a) Non-fluorescent fluid inclusions in barite observed with transmitted light (left) and UV light (right). **b-d)** Fluorescent FI in barite observed with transmitted light (left) and UV light (right). **Abbreviations:** B = bubble, L = liquid, LHC = liquid hydrocarbon, VHC = gaseous hydrocarbon.

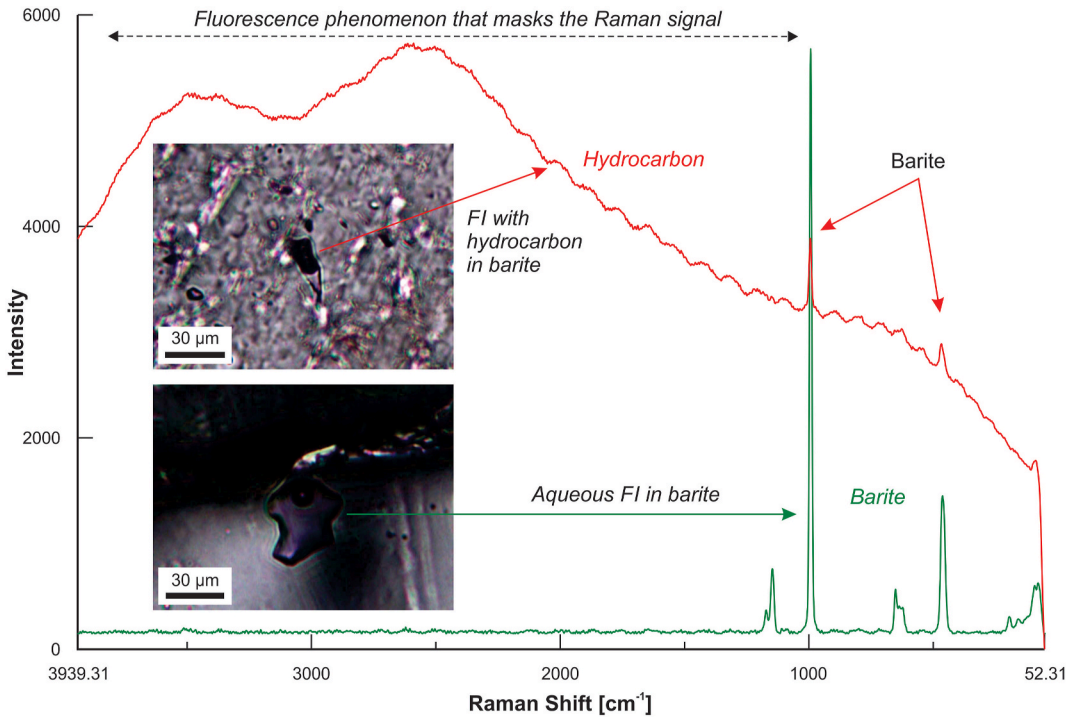

Fig. 12. Raman spectra of aqueous (green) and hydrocarbon-bearing (red) FI. In the latter spectrum, the strong masking effect of the fluorescence of hydrocarbons on the Raman signal is recognized. (For interpretation of the references to color in this figure legend, the reader is referred to the Web version of this article.)

Table 3
Fluid inclusion results of barite crystals from the Colipilli area (Neuquén Basin, Argentina).

Type of deposit	Bed-type	Vein-type
Type of inclusion	Liquid + Gas	Liquid + Gas
Number of measurements	16	20
Initial melting temperature (T_{im}) range	−44.0/−21.1 °C	−52.0/−23.3 °C
Final melting temperature (T_{fm}) range	−4.5/−0.1 °C	−5.3/−0.3 °C
Homogenization temperature (T_h) range	156.2–176.0 °C	163.0–280.6 °C
Salinity range (wt.% NaCl equiv.)	0.2–7.2	0.5–8.3

Table 4
Summary of the main characteristics of the barite-polymetallic deposits of the Colipilli area (Neuquén Basin, Argentina).

Type of deposit	Bed-type	Vein-type
Host rock	Sedimentary rocks of the Huitrín Formation and igneous rocks of the Naunauco Group.	Sedimentary rocks of the Vaca Muerta, Mulichinco, Agrio and Huitrín formations and igneous rocks of the Colipilli Formation.
Ore mineralogy	Fine barite crystals	Coarse barite crystals
Gangue mineralogy	Fe-oxyhydroxides with minor proportions of Pb-sulfides.	Fe-oxyhydroxides and subordinate sulfides of Pb, Fe, Cu and Zn.
Texture	Zebra	Breccia
Alteration	Kaolinitization	Silicification
Mineral chemistry	$Bar_{93.76\%}$ $Cel_{3.14\%}$ $Anh_{0.10\%}$	$Bar_{97.23\%}$ $Cel_{2.73\%}$ $Anh_{0.04\%}$
Mean homogenization temperature	162.2 °C	241.0 °C
Salinity range (wt. % NaCl equiv.)	0.2–7.2	0.5–8.3
Occurrence of hydrocarbons	Yes	Yes

Bar = barite, Cel = celestite, Anh = anhydrite.

These hydrothermal fluids also promoted the interaction with hydrocarbon fluids present in the sedimentary pile or expelled from source rocks affected by the thermal increase. The fluids could have migrated through the carbonate rocks of the Chorreado and Troncoso Superior members (Huitrín Formation). The replacement processes of carbonate bands by sulphates with different proportions of Ba and Sr were developed when physicochemical conditions were favorable. These processes generated the zebra texture that characterizes the bed-type deposits. The progressive somerization of the inorganic and organic hydrothermal fluids and the increasing influence of meteoric waters are reflected in the lower homogenization temperatures (T_h) and salinities of barites from the bed-type deposits (Fig. 14).

7.2. Implications in the petroleum system

The studies carried out by Cruz et al. (1996) on the thermal maturity of the source rock samples (Vaca Muerta and Agrio formations) from the southern sector of the Chos Malal Fold and Thrust Belt (north of the Colipilli area) and those performed in recovered cuttings from the BS. Nq.ChE.x-1 well (Chapúa Este, Fig. 1c), indicated a thermal maturity much higher than that provided by the output of the model obtained using a "standard" heat regime for the area. For that reason, Cruz et al. (1996) put forward a thermal anomaly during the Late Cretaceous–Tertiary, which would have increased the heat flow in the area. Thus, a better match between the modeled and measured data is possible, considering that the alternative of significant editing of the burial history to force the high maturity pattern was not a realistic scenario. In concordance with this model, the concomitant establishment of the volcanic arc in the Colipilli area, represented by lava flows, sills, laccoliths, stocks and dykes of the Naunauco Group, could have generated the necessary conditions to increase the temperature. This heating activated the convective cells that mobilized the connate waters and allowed the circulation and leaching of elements from the entire highly reactive sedimentary pile (Fig. 14). In this context, the organic matter present in the source rocks recognized in the area could have cracked generating fluid phases which would have migrated with the

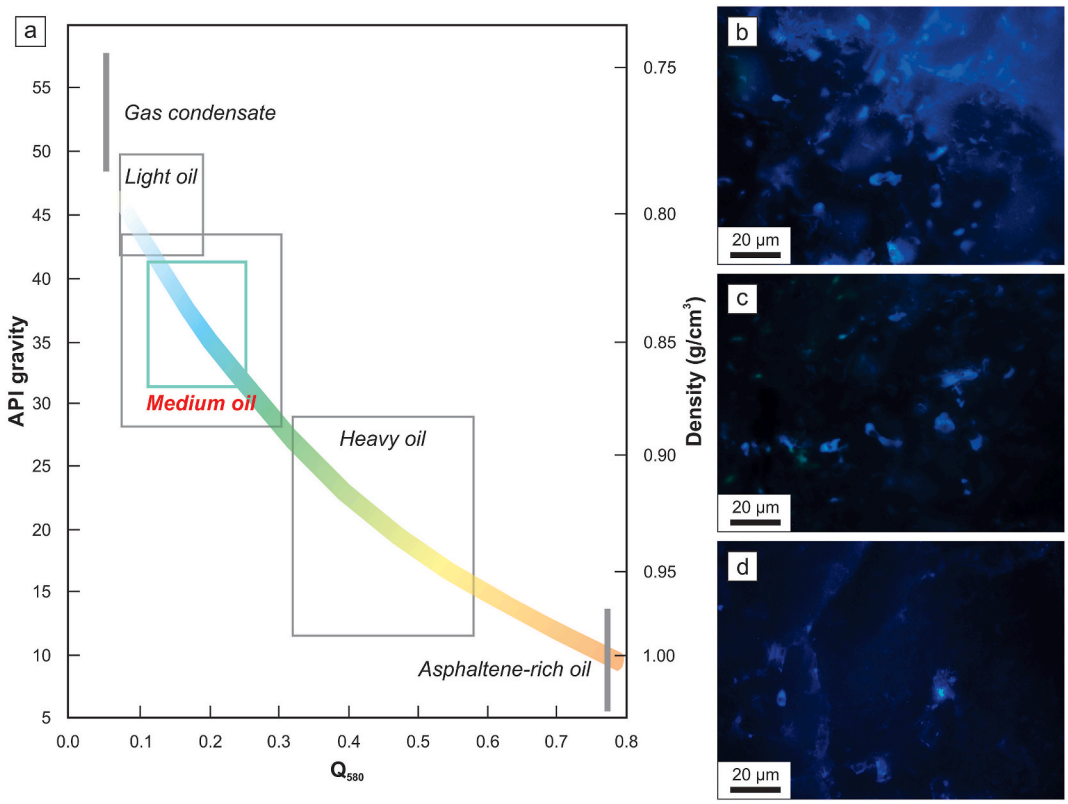

Fig. 13. a) Correlation diagram between density, API, Q580 (fluorescence degree quantification index) and color of UV fluorescence on hydrocarbons (modified from Kihle et al., 2012). The field of the identified hydrocarbon phase in barites from the Colipilli area is highlighted in blue. **b, c)** Fluorescent FI in barites from vein-type deposits. **d)** Fluorescent FI in barites from bed-type deposits. (For interpretation of the references to color in this figure legend, the reader is referred to the Web version of this article.)

connate waters. Another possibility is that hydrocarbons previously generated would have migrated into that aqueous phases until its entrapment during the barite crystallization. The kerogen transformation rate (TR) maps for the bottom of the Vaca Muerta Formation in the fold and thrust belts of the region at the end of the Neuquén Group deposition shows TR values of 60–80% (Legarreta et al., 2005). Thus, it is possible that the Naunauco Group heat effect was complementary and second-order in the maturation of the organic matter in this area. Regarding the Agrio Formation source rock, its maturation process has been more moderated and significantly much later compared to the Vaca Muerta Formation (Legarreta et al., 2005). Therefore, the invoked influence of a magmatic process could have had a more significant influence on the conversion of the Agrio Formation kerogen into hydrocarbons.

The existence of a thermal gradient anomaly during the Naunauco Group emplacement could also be supported by the thermal history modeled by Rojas Vera et al. (2015) for the western sector of the Colipilli area (obtained from an apatite fission track analyses of the Mulichinco Formation). According to these authors, the modeled sample experienced maximum temperatures between 100 and 160 °C, with best results between 140 and 155 °C. In this sense, even assuming a maximum sedimentary thickness of 3850 m deposited over the Mulichinco Formation (2050 m and 800 m for the Agrio and Rayoso formations, respectively, plus a maximum of 1000 m for the Neuquén Group; Rojas Vera et al., 2015), an abnormal thermal gradient (>30 °C/km) needs to be considered to reach the best results obtained by these authors. On the other hand, if we consider what is observed in the Chos Malal area, where the Agrio Formation thickness is close to 1000 m (Cruz et al., 1996), even more, an abnormal gradient is necessary.

8. Conclusions

Our study focuses on the hydrocarbon-bearing barite-polymetallic deposits of the Colipilli area, Neuquén Basin, Argentina, and the thermal anomaly associated with magmatic activity. The results presented in this work show that the study area and the involved rocks and barite deposits correspond to an atypical petroleum system, that is, related to igneous activity (Atypical Igneous Petroleum Systems according to Delpino and Bermúdez, 2009). The heat influx provided by the magmatism of the Naunauco Group (Late Cretaceous–Paleocene) induced the circulation of inorganic and organic fluids of connate origin through the Early Cretaceous sedimentary pile. At the same time, the circulation of these hydrothermal fluids promoted the leaching of metallic and non-metallic elements from the sedimentary pile and also the host rock maturation by increasing the thermal gradient. As a result of these processes, numerous barite occurrences were formed in this sector of the basin. During its crystallization, barite trapped fluids with variable hydrocarbon contents. In this geological context, it is also possible that part of the oil produced in the oilfields located east of the Colipilli area could have migrated from here. On the other hand, the igneous rocks of Late Cretaceous–Paleocene age of the Neuquén Basin could have acted as potential reservoirs that should be explored in the future.

The genetic model for the Colipilli barite deposits could have important implications both for the thermal evolution knowledge of the area and for contributing to adjust the models of the Neuquén Basin petroleum systems. The information generated in this type of study contributes to obtain a more realistic paleo-geothermal gradient for fold and thrust belts, avoiding inaccurate thickness estimates.

Finally, the use of fluid inclusions microthermometry, together with UV fluorescence techniques and Raman spectroscopy, proves to be a very valuable tool in the characterization and prospecting of petroleum

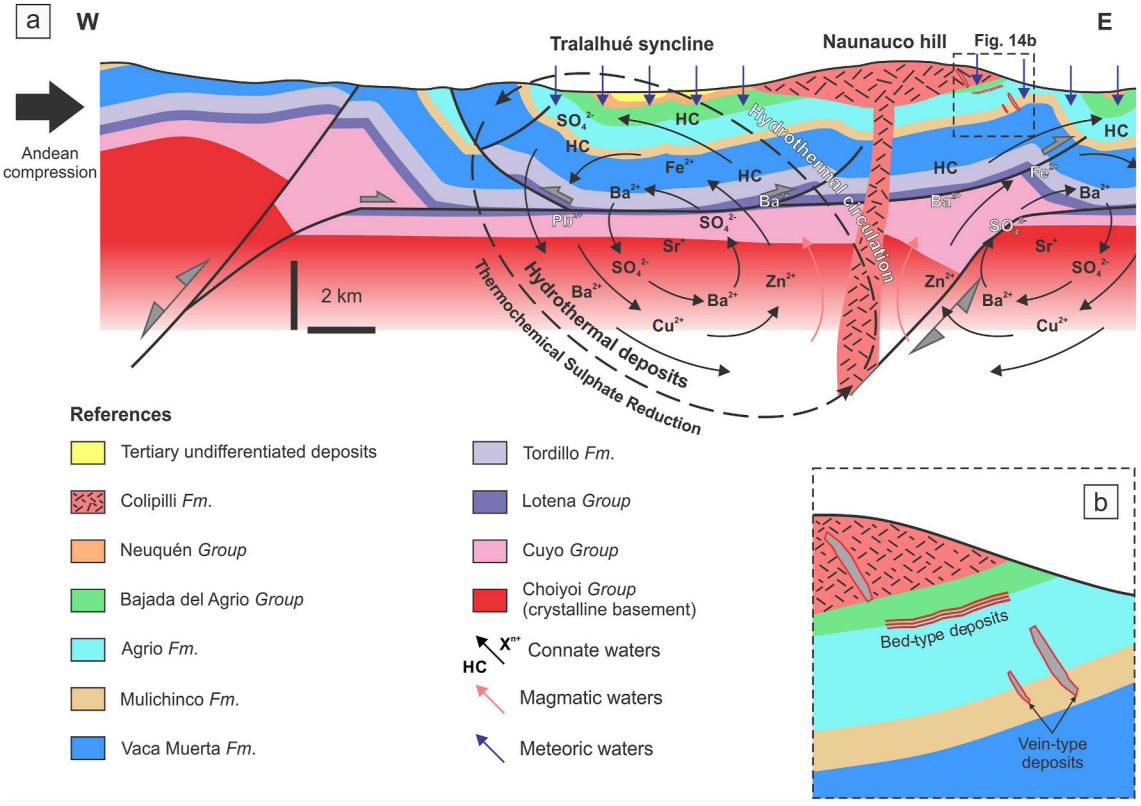

Fig. 14. Structural cross-section scheme of Naunauco hill (redrawn and modified from Zamora Valcarce (2007) and Rojas Vera et al. (2015)) showing the evolutionary model of mineralizing fluids for the Colipilli area. The black arrows represent the connate waters convectively mobilized by the heat contributed by the Late Cretaceous–Paleocene magmatism. The chemical symbols represent the elements and compounds leached and mobilized into the sequence (including hydrocarbons, HC). The red and blue arrows represent the magmatic (not significant) and meteoric (important at higher stratigraphic levels) waters, respectively. (For interpretation of the references to color in this figure legend, the reader is referred to the Web version of this article.)

systems.

Credit author statement

Melisa A. Salvioli: Conceptualization, Methodology, Investigation, Writing - Original Draft, Writing - Review & Editing, Visualization. **Carlos A. Ballivián Justiniano**: Investigation, Writing - Original Draft, Writing - Review & Editing, Visualization. **María F. Lajoinie**: Investigation, Writing - Original Draft, Writing - Review & Editing. **Hernán G. de la Cal**: Investigation, Writing - Original Draft, Writing - Review & Editing. **Remigio Ruiz**: Resources, Investigation, Writing - Original Draft. **Nora N. Cesaretti**: Resources, Investigation, Supervision, Writing - Original Draft. **Mabel E. Lanfranchini**: Supervision, Investigation, Writing - Original Draft, Funding acquisition.

Declaration of competing interest

The authors declare that they have no known competing financial interests or personal relationships that could have appeared to influence the work reported in this paper.

Acknowledgements

We would like to acknowledge Raúl E. de Barrio and Rodrigo I. Escobar for their invaluable help during this study, and Qinhong Hu and two anonymous reviewers for their constructive comments that helped improve the original manuscript. We also like to acknowledge Friedemann U.M. Baur for the editorial handling. This study was supported by research fellowships awarded to the first three authors by the *Consejo Nacional de Investigaciones Científicas y Técnicas* (CONICET) of Argentina. Research grants awarded by the CONICET (PIP-0285), the *Universidad Nacional de La Plata* (11N 540 and 11N 692) and the Society of Economic Geologists (SEG) also supported this study.

References

Agirrezabala, L.M., Permanyer, A., Suárez-Ruiz, I., Dorronsoro, C., 2014. Contact metamorphism of organic-rich mudstones and carbon release around a magmatic sill in the Basque-Cantabrian Basin, western Pyrenees. Org. Geochem. 69, 26–35.

Aguirre-Urreta, B., Tunik, M., Naipauer, M., Pazos, P., Ottone, E., Fanning, M., Ramos, V. A., 2011. Malargüe group (Maastrichtian–Danian) deposits in the Neuquén andes, Argentina: implications for the onset of the first atlantic transgression related to western Gondwana break-up. Gondwana Res. 19, 482–494.

Alberdi-Genolet, M., Cavallaro, A., Hernández, N., Crosta, D.E., Martinez, L., 2013. Magmatic events and sour crude oils in the Malargüe area of the Neuquén Basin, Argentina. Mar. Petrol. Geol. 43, 48–62.

Angelelli, V., Schalamuk, I.B., Arrospide, A., 1976. Los yacimientos no metalíferos y rocas de aplicación de la región Patagonia-Comahue, vol. 17. Secretaría de Estado de Minería, Buenos Aires. Anales.

Bodnar, R.J., 1990. Petroleum migration in the Miocene Monterey Formation, CA, USA: constraints from fluid-inclusion studies. Mineral. Mag. 54, 295–304.

Bolonin, A.V., Nikiforov, A.V., 2014. Intermediate sulfates in barite-celestite isomorphic series: composition and mode of occurrence. Geol. Ore Deposits 56, 302–314.

Bracaccini, I.O., 1970. Rasgos tectónicos de las acumulaciones mesozoicas en las provincias de Mendoza y Neuquén, República Argentina. Rev. Asoc. Geol. Argent. 25, 275–282.

Brisson, I.E., 2015. Sistemas petroleros de la Cuenca neuquina. In: Ponce, J.J., Montagna, A.O., Carmona, N. (Eds.), Geología de la Cuenca Neuquina y sus sistemas petroleros: una mirada integradora desde los afloramientos al subsuelo. Universidad Nacional de Río Negro & Fundación YPF, Viedma, pp. 22–35.

Brisson, I.E., Fasola, M.E., Villar, H.J., 2020. Organic Geochemical Patterns of Vaca Muerta Shale, Neuquén Basin, Argentina. Search and Discovery article #11302.

Brodtkorb, M.K., Ramos, V.A., Ametrano, S., 1975. Los yacimientos estratoligados de celestina-baritina de la Formación Huitrín y su origen evaporítico. Provincia del Neuquén. Argentina. In: 2° Congreso Iberoamericano de Geología Económica, vol. 2. Actas, Buenos Aires, pp. 143–168.

Brodtkorb, M.K., Schalamuk, I.B., Barbieri, M., Ametrano, S., Fernández, R.R., Etcheverry, R.O., Aragón, E., 1985. Los yacimientos de baritina y celestina del

Mesozoico de Mendoza y Neuquén. Argentina. In: 4° Congreso Geológico Chileno, Antofagasta, Actas, vol. 2, pp. 156–183.
Burke, E.A.J., 2001. Raman microspectrometry of fluid inclusions. Lithos 55, 139–158.
Burkhard, A., 1978. Baryt-Celestin and ihre Mischkristalle aus Schweizer Alpen and Jura. Schweizerische mineralogische und petrographische Mitteilungen 58, 1–96.
Burrus, R.C., 1981. Hydrocarbon fluid inclusions in studies on sedimentary diagenesis. In: Hollister, L.S., Crawford, M.L. (Eds.), Fluid Inclusions: Applications to Petrology, pp. 138–154. Mineralogical Association of Canada, Short Course Volume 6, Quebec.
Carbone, O., Vergani, G., Giusiano, A., Raviola, M., 2018. A un siglo del descubrimiento de petróleo en Neuquén (1918-2018) perspectivas sobre la matriz energética Argentina. In: 10° Congreso de Exploración y Desarrollo de Hidrocarburos, Mendoza, Sesiones Especiales, pp. 3–20.
Cobbold, P.R., Rossello, E.A., 2003. Aptian to recent compressional deformation, foothills of the Neuquén Basin, Argentina. Mar. Petrol. Geol. 20, 429–443.
Cobbold, P.R., Ruffet, G., Leith, L., Loseth, H., Rodrgues, N., Leanza, H.A., Zanella, A., 2014. Radial patterns of bitumen dykes around Quaternary volcanoes, provinces of northern Neuquén and southernmost Mendoza, Argentina. J. S. Am. Earth Sci. 56, 454–467.
Collao, S., 1998. Inclusiones fluidas en celestinas de los yacimientos de la Formación Huitrín, Provincia de Neuquén, Argentina. In: 40° Congresso Brasileiro de Geologia, Belo Horizonte, Anais, p. 174.
Collao, S., Brodtkorb, M.K., Etcheverry, R.O., 1997. Inclusiones fluidas en baritas recristalizadas de los yacimientos de la provincia de Neuquén, Argentina. In: 8° Congreso Geológico Chileno, Antofagasta, Actas, vol. 2, pp. 901–905.
Cruz, C.E., Villar, H.J., Muñoz, G.N., 1996. Los sistemas petroleros del Grupo Mendoza en la Fosa de Chos Malal, Cuenca Neuquina, Argentina. In: 13° Congreso Geológico Argentino y 3° Congreso de Exploración de Hidrocarburos, Buenos Aires, Actas, vol. 1, pp. 45–60.
de Barrio, R.E., Del Blanco, M.A., García, M., Martin-Izard, A., 2009. Estructuras estromatolíticas y su relación con las mineralizaciones de Ba-Sr emplazadas en la Formación Huitrín, Cuenca Neuquina. In: 9° Congreso Argentino de Geología Económica, pp. 45–51. Catamarca, Actas.
de Barrio, R.E., Del Blanco, M.A., Colombo, F., Martín-Izard, A., Ramis, A.M., Curci, M. V., 2016. Variaciones composicionales en baritinas y celestinas de depósitos de Ba-Sr emplazados en la secuencia jurásico-cretácica de la provincia del Neuquén. Acta Geol. Lilloana 28, 117–123.
de Barrio, R.E., Etcheverry, R.O., Del Blanco, M.A., Domínguez, E.A., Recio Hernández, C., Escobar, R.I., Salvioli, M.A., 2014. Nuevos datos y esquemas genéticos de los depósitos barítico-celestínicos vinculados a la secuencia jurásico-cretácica de la Cuenca Neuquina en la provincia del Neuquén. Rev. Asoc. Geol. Argent. 71, 184–200.
Deer, W.A., Howie, R.A., Zussman, J., 1992. An Introduction to the Rock-Forming Minerals. Wiley, New York.
Dellapé, D.A., Mombrú, C., Pando, G.A., Riccardi, A.C., Uliana, M.A., Westermann, G.E., 1978. Edad y correlación de la Formación Tábanos en Chacay Melehue y otras localidades de Neuquén y Mendoza. In: Con consideraciones sobre la distribución y significado de las sedimentitas Lotenianas, vol. 5. Obra Centenario del Museo de La Plata (Paleontología), pp. 81–105.
Delpino, D.H., Bermúdez, A.M., 2009. Petroleum systems including unconventional reservoirs in intrusive igneous rocks (sills and laccoliths). Lead. Edge 28, 804–811.
Dubessy, J., Ramboz, C., 1986. The history of organic nitrogen from early diagenesis to amphibolite facies: mineralogical, chemical, mechanical and isotopic implications. 5° International Symposium on Water–Rock Interaction. Reykjavik, Extended Abstracts, pp. 170–174.
Escobar, R.I., 2016. Geología y génesis de las mineralizaciones barito-celestínicas asociadas a la secuencia cretácia entre las localidades Bajada del Agrio y Chos Malal, provincia del Neuquén. Ph.D. thesis, Universidad Nacional de La Plata.
Escobar, R.I., de Barrio, R.E., Etcheverry, R.O., Recio Hernández, C., 2013a. Características litoestratigráficas y geoquímicas de los depósitos celesto-baríticos del Grupo Continental, Provincia del Neuquén. 10° Congreso Argentino de Geología Económica, pp. 9–25. San Juan, Actas.
Escobar, R.I., Salvioli, M.A., de Barrio, R.E., Lanfranchini, M.E., Etcheverry, R.O., 2013b. Texturas cebradas asociadas a las mineralizaciones de Ba-Sr alojadas en la Formación Huitrín, entre Chos Malal y Bajada del Agrio, Neuquén. 11° Congreso de Mineralogía y Metalogenia, pp. 211–216. Salta, Actas.
Franzese, J.R., Spalletti, L.A., 2001. Late Triassic–Early Jurassic continental extension in southwestern Gondwana: tectonic segmentation and pre-break-up rifting. J. S. Am. Earth Sci. 14, 257–270.
Franzese, J.R., Spalletti, L.A., Gómez Pérez, I., Macdonald, D., 2003. Tectonic and paleoenvironmental evolution of Mesozoic sedimentary basins along the Andean foothills of Argentina (32°–54°S). J. S. Am. Earth Sci. 16, 81–90.
Goldstein, R.H., Reynolds, T.J., 1994. Systematics of fluid inclusions in diagenetic minerals. SEPM Society for Sedimentary Geology ume 31. Broken Arrow.
Groeber, P., 1946. Observaciones geológicas a lo largo del meridiano 70°. 1. Hoja Chos Malal. Rev. Asoc. Geol. Argent. 1, 177–208.
Gutiérrez Pleimling, A.R., 1991. Estratigrafía de la Formación Huitrín: un estudio puntual sobre la ruta Nacional N° 40, provincia del Neuquén. Bol. Inf. Pet. (1924) 8, 85–100.
Hayase, K., Bengochea, A.L., 1975. Consideraciones sobre la génesis de algunos yacimientos de baritina-celestina; provincia de Neuquén; República Argentina. In: 2° Congreso Iberoamericano de Geología Económica, vol. 2. Actas, Buenos Aires, pp. 295–314.
Howell, J.A., Schwarz, E., Spalletti, L.A., Veiga, G., 2005. The Neuquén Basin: an overview. In: Veiga, G.D., Spalletti, L.A., Howell, J.A., Schwarz, E. (Eds.), The Neuquén Basin, Argentina: A Case Study in Sequence Stratigraphy and Basin Dynamics, vol. 252. Geological Society, Special Publications, London, pp. 1–14.
Kay, S.M., Copeland, P.C., 2006. Early to middle Miocene back-arc magmas of the Neuquén Basin: geochemical consequences of slab shallowing and the westward drift of South America. In: Kay, S.R., Ramos, V.A. (Eds.), Evolution of an Andean Margin: A Tectonic and Magmatic View from the Andes to the Neuquén Basin (35°-39°S Lat). Geological Society of America, Special Paper 497, Boulder, pp. 19–60.
Kihle, J., Hurum, J.H., Liebe, L., 2012. Preliminary results on liquid petroleum occurring as fluid inclusions in intracellular mineral precipitates in the vertebrate of *Pliosaurus funkei*. Norw. J. Geol. 92, 341–352.
Leal, P., Mateo, P., 2015. Paragénesis y microtermometría de las manifestaciones de baritina del anticlinal de Chorriaca, provincia del Neuquén. Rev. Asoc. Geol. Argent. 72, 195–209.
Leanza, H.A., 1992. Estratigrafía del Paleozoico y Mesozoico anterior a los Movimientos Intermálmicos en la comarca del Cerro Chachil, provincia del Neuquén, Argentina. Rev. Asoc. Geol. Argent. 45, 272–299.
Leanza, H.A., Repol, D., Hugo, C.H., Sruoga, P., 2006. Hoja Geológica 3769-31, Chorriaca, Provincia del Neuquén, vol. 354. Instituto de Geología y Recursos Minerales & Servicio Geológico Minero Argentino, Boletín, Buenos Aires.
Legarreta, L., Uliana, M.A., 1991. Jurassic-marine oscillations and geometry of back-arc basin fill, central Argentine andes. In: MacDonald, D.I.M. (Ed.), Sedimentation, Tectonics and Eustasy: Sea-Level Changes at Active Margins, vol. 12. International Association of Sedimentologists, Special Publications, Gent, pp. 429–450.
Legarreta, L., Uliana, M.A., 1999. Facies sedimentarias. El jurásico y cretácico de la Cordillera principal y la Cuenca neuquina. In: Caminos, R. (Ed.), Geología Argentina, vol. 29. Instituto de Geología y Recursos Minerales, Anales, Buenos Aires, pp. 399–432.
Legarreta, L., Villar, H.J., Cruz, C.E., Laffitte, G.A., Varadé, R., 2008. Revisión integrada de los sistemas generadores, estilos de migración-entrampamiento y volumetría de hidrocarburos en los distritos productivos de la Cuenca Neuquina, Argentina. In: Cruz, C.E., Rodríguez, J.F., Hechem, J.J., Villar, H.J. (Eds.), Sistemas Petroleros de las Cuencas Andinas. 7° Congreso de Exploración y Desarrollo de Hidrocarburos. Mar del Plata, 79–108.
Legarreta, L., Villar, H.J., Laffitte, G.A., Cruz, C.E., Vergani, G., 2005. Cuenca neuquina. In: Chebli, G.A., Cortiñas, J.S., Spaletti, L.A., Legarreta, L., Vallejo, E.L. (Eds.), Simposio Frontera Exploratoria de la Argentina. 6° Congreso de Exploración y Desarrollo de Hidrocarburos, Mar del Plata, pp. 233–250.
Llambías, E.J., Aragón, E., 2011. Volcanismo paleógeno. In: Leanza, H.A., Arregui, C., Carbone, O., Danieli, J.C., Vallés, J.M. (Eds.), Geología y Recursos Naturales de la provincia del Neuquén. Relatorio del 18° Congreso Geológico Argentino (Neuquén), pp. 265–274. Buenos Aires.
Llambías, E.J., Malvicini, L., 1978. Geología, petrología y metalogénesis del área de Colipilli, provincia del Neuquén, República Argentina. Rev. Asoc. Geol. Argent. 33, 257–276.
Llambías, E.J., Rapela, C.W., 1987. Las vulcanitas de Colipilli y sus relaciones con las provincias volcánicas del Terciario inferior de Neuquén-Mendoza y Patagonia. In: 10° Congreso Geológico Argentino (San Miguel de Tucumán), Buenos Aires, Actas, vol. 4, pp. 249–251.
Llambías, E.J., Rapela, C.W., 1989. Las volcanitas de Colipilli, Neuquén (37°S) y su relación con otras unidades paleógenas de la cordillera. Rev. Asoc. Geol. Argent. 44, 224–236.
Machel, H.G., 1998. Gas souring by thermochemical sulfate reduction at 140°C: discussion. AAPG (Am. Assoc. Pet. Geol.) Bull. 82, 1870–1873.
Machel, H.G., 2001. Bacterial and thermochemical sulfate reduction in diagenetic settings – old and new insights. Sediment. Geol. 140, 143–175.
Magoon, L.B., Dow, W.G., 1994. The petroleum system. In: Magoon, L.B., Dow, W.G. (Eds.), The Petroleum System – from Source to Trap. AAPG Memoir 60, Tusla, pp. 3–24.
Méndez, V., Zanettini, J.C.M., Zappettini, E.O., 1995. Geología y metalogénesis del Orógeno Andino Central, República Argentina, vol. 23. Dirección Nacional del Servicio Geológico, Anales, Buenos Aires.
Nielsen, P., Swennen, R., Muchez, P.H., Keppens, E., 1998. Origin of dinantian zebra dolomites south of the brabant-wales Massif, Belgium. Sedimentology 45, 727–743.
Ramos, V.A., 1978. Estructura. In: Rolleri, E.O. (Ed.), Geología y Recursos Naturales de la provincia del Neuquén. Relatorio del 7° Congreso Geológico Argentino (Neuquén), pp. 233–237. Buenos Aires.
Ramos, V.A., 1998. Estructura del sector Occidental de la Faja Plegada y Corrida del Agrio, Cuenca Neuquina, Argentina. In: 10° Congreso Geológico Latinoamericano y 6° Congreso Nacional de Geología Económica, Buenos Aires, Actas, vol. 2, pp. 105–110.
Ramos, V.A., Barbieri, M., 1988. El volcanismo Cenozoico de Huantraico: edad y relaciones isotópicas iniciales, provincia del Neuquén. Rev. Asoc. Geol. Argent. 43, 210–223.
Rapela, C.W., Llambías, E.J., 1985. La secuencia andesítica terciaria de Andacollo, Neuquén, Argentina. In: 4° Congreso Geológico Chileno, Antofagasta, Actas, vol. 4, pp. 458–488.
Repol, D., Leanza, H.A., Sruoga, P., Hugo, C.A., 2002. Evolución tectónica del Cenozoico de la comarca de Chorriaca, Provincia del Neuquén, Argentina. In: 15° Congreso Geológico Argentino (El Calafate), Buenos Aires, Actas, vol. 3, pp. 200–205.
Riecker, R.E., 1962. Hydrocarbon fluorescence and migration of petroleum. AAPG (Am. Assoc. Pet. Geol.) Bull. 46, 60–75.
Rocha, E., Brisson, I.E., Fasola, M.E., 2018. Modelado de sistemas petroleros a lo largo de la Faja Plegada de la Cuenca Neuquina. 10° Congreso de Exploración y Desarrollo de Hidrocarburos, pp. 301–313. Mendoza, Actas.
Rodríguez Monreal, F., Villar, H.J., Baudino, R., Delpino, D., Zencicha, S., 2009. Modeling an atypical petroleum system: a case study of hydrocarbon generation, migration and accumulation related to igneous intrusions in the Neuquén Basin, Argentina. Mar. Petrol. Geol. 26, 590–605.

Roedder, E., 1963. Studies of fluid inclusions II: freezing data and their interpretation. Econ. Geol. 58, 167–211.
Roedder, E., 1984. Fluid inclusions. In: Reviews in Mineralogy, vol. 12. Mineralogical Society of America, Chantilly.
Rojas Vera, E.A., 2011. Evolución tectónica de los Andes Centrales Australes (36-39°S): el caso de un orógeno reactivado extensionalmente, la Fosa de Loncopué. Ph.D. thesis, Universidad de Buenos Aires.
Rojas Vera, E.A., Mescua, J., Folguera, A., Becker, T.P., Sagripanti, L., Fennell, L., Orts, D., Ramos, V.A., 2015. Evolution of the Chos Malal and Agrio fold and thrust belts, Andes of Neuquén: insights from structural analysis and apatite fission track dating. J. S. Am. Earth Sci. 64, 418–433.
Salvioli, M.A., 2017. Geología y génesis de los depósitos barítico-polimetálicos (Ba-Fe-Pb-Cu-Zn-Mn) del área de Colipilli, sector centro-Occidental de la Cuenca Neuquina. Ph.D. thesis, Universidad Nacional de La Plata.
Salvioli, M.A., Lajoinie, M.F., Cesaretti, N.N., Lanfranchini, M.E., de la Cal, H.G., Ruiz, R., 2018. Registro de hidrocarburos en los depósitos barito-polimetálicos del área de Colipilli, sector centro-Occidental de la Cuenca Neuquina, Argentina. 10° Congreso de Exploración y Desarrollo de Hidrocarburos, pp. 329–344. Mendoza, Actas.
Seal II, R.R., 2006. Sulfur isotope geochemistry of sulfide minerals. Rev. Mineral. Geochem. 61, 633–677.
Senger, K., Millett, J., Planke, S., Ogata, K., Eide, C.H., Festøy, M., 2017. Effects of igneous intrusions on the petroleum system: a review. First Break 35, 47–56.
Spacapan, J.B., D'Odorico, A., Palma, O., Gallandd, O., Rojas Vera, E., Ruiz, R., Leanza, H.A., Medialdea, A., Manceda, R., 2020. Igneous petroleum systems in the Malargüe fold and thrust belt, Río Grande Valley area, Neuquén Basin, Argentina. Mar. Petrol. Geol. 111, 309–311.
Stasiuk, L.D., Snowdon, L.R., 1997. Fluorescence micro-spectrometry of synthetic and natural hydrocarbon fluid inclusions: crude oil chemistry, density and application to petroleum migration. Appl. Geochem. 12, 229–241.
Stipanicic, P.N., Rodrigo, F., Baulies, O.L., Martínez, C.G., 1968. Las formaciones presenonianas del denominado Macizo Nordpatagónico y regiones adyacentes. Rev. Asoc. Geol. Argent. 23, 367–388.
Tsui, T.F., 1990. Characterizing fluid inclusion oils via UV fluorescence microspectrophotometry – a method for projecting oil quality and constraining oil migration history. AAPG (Am. Assoc. Pet. Geol.) Bull. 74, 781.
Tunik, M., Folguera, A., Naipauer, M., Pimentel, M., Ramos, V.A., 2010. Early uplift and orogenic deformation in the Neuquén Basin: constraints on the Andean uplift from U–Pb and Hf isotopic data of detrital zircons. Tectonophysics 489, 258–273.
Vanderginste, V., Swennen, R., Gleeson, S.A., Ellam, R.M., Osadetz, K., Roure, F., 2005. Zebra dolomitization as a result of focused fluid flow in the Rocky Mountains Fold and thrust belt, Canada. Sedimentology 52, 1067–1095.
Vergani, G.D., Tankard, A.J., Belotti, H.J., Welsink, H.J., 1995. Tectonic evolution and paleogeography of the Neuquén basin, Argentina. In: Tankard, A.J., Suárez, R., Welsink, H.J. (Eds.), Petroleum Basins of South America, vol. 62. American Association of Petroleum Geologists, Memoire, Tulsa, pp. 383–402.
Weaver, C., 1931. Paleontology of the Jurassic and Cretaceous of West Central Argentina, vol. 1. University of Washington, Memoire, Seattle, pp. 1–469.
Zamora Valcarce, G., 2007. Estructura y cinemática de la faja plegada del Agrio. Ph.D. thesis, Universidad de Buenos Aires.
Zamora Valcarce, G., Zapata, T.R., Ramos, V.A., 2011. La faja plegada y corrida del Agrio. In: Leanza, H.A., Arregui, C., Carbone, O., Danieli, J.C., Vallés, J.M. (Eds.), Geología y Recursos Naturales de la provincia del Neuquén. Relatorio del 18° Congreso Geológico Argentino (Neuquén), pp. 367–374. Buenos Aires.
Zamora Valcarce, G., Zapata, T.R., del Pino, D., Ansa, A., 2006. Structural evolution and magmatic characteristics of the Agrio fold-and-thrust belt. In: Kay, S.R., Ramos, V.A. (Eds.), Evolution of an Andean Margin: A Tectonic and Magmatic View from the Andes to the Neuquén Basin (35°-39°S Lat), vol. 497. Geological Society of America, Special Paper, Boulder, pp. 125–145.
Zamora Valcarce, G., Zapata, T.R., Ramos, V.A., Rodríguez, F., Bernardo, L.M., 2009. Evolución tectónica del Frente Andino en Neuquén. Rev. Asoc. Geol. Argent. 65, 192–203.
Zapata, T.R., Folguera, A., 2006. Tectonic evolution of the andean fold and thrust belt of the southern Neuquén Basin, Argentina. In: Veiga, G.D., Spalletti, L.A., Howell, J.A., Schwarz, E. (Eds.), The Neuquén Basin, Argentina: A Case Study in Sequence Stratigraphy and Basin Dynamics, vol. 252. Geological Society, Special Publications, London, pp. 37–56.
Zapata, T.R., Brisson, I.E., Dzelalija, F., 1999. La estructura de la faja plegada y corrida andina en relación con el control del basamento de la Cuenca Neuquina. Bol. Inf. Pet. (1924) 60, 113–121.
Zapata, T.R., Córsico, S., Dzelalija, F., Zamora Valcarce, G., 2002. La faja plegada y corrida del Agrio: análisis estructural y su relación con los estratos terciarios de la Cuenca Neuquina, Argentina. 5° Congreso de Exploración y Desarrollo de Hidrocarburos. Mar del Plata, electronic abstracts.